MULTIMODAL NEURAL CORRELATES OF CHILDHOOD PSYCHOPATHOLOGY

Valeria Kebets[1,2,3,4], Camille Piguet[5,6], Jianzhong Chen[2,3,4], Leon Qi Rong Ooi[2,3,4], Matthias Kirschner[1,7], Vanessa Siffredi[8,9,10], , Bratislav Misic[1], B.T. Thomas Yeo[2,3,4,11,12*], Boris C. Bernhardt[1*]

[1] *McConnell Brain Imaging Centre, Montreal Neurological Institute, McGill University, Montreal, QC, Canada*

[2] *Centre for Sleep and Cognition & Centre for Translational MR Research, Yong Loo Lin School of Medicine, National University of Singapore, Singapore*

[3] *Department of Electrical and Computer Engineering, National University of Singapore, Singapore*

[4] *N.1 Institute for Health & Institute for Digital Medicine, National University of Singapore, Singapore*

[5] *Young Adult Unit, Psychiatric Specialities Division, Geneva University Hospitals and Department of Psychiatry, Faculty of Medicine, University of Geneva, Switzerland*

[6] *Adolescent Unit, Division of General Paediatric, Department of Paediatrics, Gynaecology and Obstetrics, Geneva University Hospitals*

[7] *Division of Adult Psychiatry, Department of Psychiatry, Geneva University Hospitals, Geneva, Switzerland*

[8] *Division of Development and Growth, Department of Paediatrics, Gynaecology and Obstetrics, Geneva University Hospitals and University of Geneva, Geneva, Switzerland*

[9] *Neuro-X Institute, Ecole Polytechnique Fédérale de Lausanne, Geneva, Switzerland*

[10] *Department of Radiology and Medical Informatics, Faculty of Medicine, University of Geneva, Switzerland*

[11] *Integrative Sciences and Engineering Programme, National University Singapore, Singapore*

[12] *Martinos Center for Biomedical Imaging, Massachusetts General Hospital, Charlestown, MA, USA*

* shared co-authorship

Corresponding authors:

Boris Bernhardt, PhD
McGill University
boris.bernhardt@mcgill.ca

BT Thomas Yeo, PhD
National University of Singapore
thomas.yeo@nus.edu.sg

ABSTRACT

Complex structural and functional changes occurring in typical and atypical development necessitate multidimensional approaches to better understand the risk of developing psychopathology. Here, we simultaneously examined structural and functional brain network patterns in relation to dimensions of psychopathology in the Adolescent Brain Cognitive Development dataset. Several components were identified, recapitulating the psychopathology hierarchy, with the general psychopathology (*p*) factor explaining most covariance with multimodal imaging features, while the internalizing, externalizing, and neurodevelopmental dimensions were each associated with distinct morphological and functional connectivity signatures. Connectivity signatures associated with the *p* factor and neurodevelopmental dimensions followed the sensory-to-transmodal axis of cortical organization, which is related to the emergence of complex cognition and risk for psychopathology. Results were consistent in two separate data subsamples, supporting generalizability, and robust to variations in analytical parameters. Our findings help in better understanding biological mechanisms underpinning dimensions of psychopathology, and could provide brain-based vulnerability markers.

KEYWORDS

psychopathology, development, transdiagnostic, multimodal imaging, multivariate, brain gradients

INTRODUCTION

Late childhood is a period of major neurodevelopmental changes (Goddings et al., 2014; Lebel and Beaulieu, 2011; Mills et al., 2021; Paus et al., 2008; Raznahan et al., 2011), which makes it particularly vulnerable for the emergence of mental illness. Indeed, about 35% of mental illnesses begin prior to age 14 (Solmi et al., 2022), motivating efforts to identify vulnerability markers of psychopathology early on (Lynch et al., 2021). This is complemented by ongoing efforts in moving towards a neurobiologically-based characterization of psychopathology. One key initiative is the Research Domain Criteria (RDoC), a transdiagnostic framework to study the neurobiological underpinnings of dimensional constructs, by integrating findings from genetics, cognitive neuroscience, and neuroimaging (Cuthbert, 2014; Insel et al., 2010). From a neurodevelopmental perspective, a transdiagnostic approach in characterizing behavioral difficulties in children and adolescents might capture a broader subset of children at risk (Astle et al., 2022; Casey et al., 2014; Jones et al., 2021; Siugzdaite et al., 2020). Such approach is also in line with continuum models, which have gained momentum in the conceptualization of psychiatric and neurodevelopmental conditions in recent years. While not without controversy, several neurodevelopmental conditions have been increasingly conceptualized as a continuum that encompasses subclinical expressions within the general population, intermediate outcomes, and a full diagnosis at the severe tail of the distribution (Abu-Akel et al., 2019; Lundström et al., 2012; Robinson et al., 2016, 2011). Such a more quantitative approach to psychopathology could capture the entire range of variation (*i.e.*, typical, subclinical, atypical) in both symptom and brain data (Insel et al., 2010; Plomin et al., 2009), and help elucidate their ties (Parkes et al., 2020).

Psychopathology can be conceptualized along a hierarchical structure, with a general psychopathology (or *p* factor) at the apex, reflecting an individual's susceptibility to develop any common form of psychopathology (Caspi et al., 2014; Kotov et al., 2017; Lahey et al., 2017). Next in this hierarchy are higher-order dimensions underpinning internalizing behaviors, such as anxiety or depressive symptoms, as well as externalizing behaviors, characterized by rule-breaking and aggressive behavior. Further, a neurodevelopmental dimension has been described to encompass symptoms with shared genetic vulnerability, such as attention deficit/hyperactivity deficit (ADHD)-related symptoms, (*e.g.*, inattention and hyperactivity), as well as clumsiness and autistic-like traits. This dimension is particularly relevant as it might underpin the normal variation in ADHD- and autism spectrum disorder

(ASD)-like traits in the general population, but also learning disabilities (Holmes et al., 2021). Recently, five dimensions of psychopathology, *i.e.,* internalizing, externalizing, neurodevelopmental, detachment, and somatoform (Michelini et al., 2019), were derived using exploratory factor analysis on parent-reported behavioral data from the Adolescent Brain Cognitive Development (ABCD) dataset, a large community-based cohort of typically developing children (Casey et al., 2018). These findings are largely consistent with the Hierarchical Taxonomy of Psychopathology (HiTOP) (Kotov et al., 2017), a dimensional classification system that aims to provide more robust clinical targets than traditional taxonomies.

Progress of neuroimaging techniques, particularly magnetic resonance imaging (MRI), has enabled the investigation of pathological mechanisms *in vivo*. To date, most neuroimaging studies to date have employed case-control comparisons between cohorts with a psychiatric diagnosis and neurotypical controls (Etkin, 2019). However, an increasing number of studies have adopted transdiagnostic neuroimaging designs in recent years (Baker et al., 2019; Elliott et al., 2018; Kebets et al., 2021, 2019; Parkes et al., 2021; Romer and Pizzagalli, 2021; Xia et al., 2018). At the level of neuroimaging measures, many studies have focused on structural metrics, such as cortical thickness, volume, surface area, or diffusion MRI derived measures of fiber architecture (Cauda et al., 2018; de Lange et al., 2019; Goodkind et al., 2015; Hettwer et al., 2022). On the other hand, there has been a rise in studies assessing functional substrates, notably work based on resting-state functional connectivity (Karcher et al., 2021; Sha et al., 2018; Xia et al., 2018). Despite increasing availability of multimodal datasets (Casey et al., 2018; Jernigan et al., 2016; Miller et al., 2016; Royer et al., 2022; Satterthwaite et al., 2016; Thompson et al., 2014; Van Essen et al., 2013), combined assessments of structural and functional substrates of psychopathology remain scarce, specifically with a transdiagnostic design.

In this context, unsupervised techniques such as partial least squares (PLS) or canonical correlation analysis, may provide a data-driven integration of different imaging measures, and allow for the identification of dimensional substrates of psychopathology along with potential neurobiological underpinnings. Recent work integrating neuroanatomical, neurodevelopmental, and psychiatric data has furthermore pointed to a particular importance of the progressive differentiation between sensory/motor systems and transmodal association cortices, also referred to as sensory-to-transmodal or sensorimotor-to-association axis of

cortical organization (Huntenburg et al., 2018; Margulies et al., 2016; Paquola et al., 2019; Park et al., 2022b; Sydnor et al., 2021). Indeed, compared to sensory and motor regions, transmodal association systems, such as the default mode network, have a long maturation time, which renders them particularly vulnerable for development of psychopathology (Paquola et al., 2019; Park et al., 2022b; Sydnor et al., 2021). Crucially, the maturation of association cortices underlies important changes in cognition, affect, and behavior, and has been suggested to highly contribute to inter-individual differences in functioning and risk for psychiatric disorders (Sydnor et al., 2021).

Here, we simultaneously delineated structural and functional brain patterns related to dimensions of psychopathology in a large cohort of children aged 9-11 years old. Children psychopathology was characterized with the parent-reported Child Behavior Checklist (CBCL)(Achenbach and Rescorla, 2013). We favored the item-based version to capture the covariation between symptoms with more granularity compared to subscales. To profile neural substrates, we combined multiple intrinsic measures of brain structure (*i.e.,* cortical surface area, thickness, volume) and functional connectivity at rest in our primary analysis. *Post hoc* analyses in smaller subsamples also incorporated diffusion-based measures of fiber architecture (*i.e.,* fractional anisotropy, mean diffusivity) and explored connectivity during tasks tapping into executive and reward processes. We expected that the synergistic incorporation of multiple brain measures may capture multiple scales of brain organization during this critical developmental moment, and thus offer sensitivity in identifying neural signatures of psychopathology dimensions. We further examined if substrates of psychopathology followed the sensory-to-transmodal axis of cortical organization. We conducted our analysis in a Discovery subsample of the ABCD cohort, and validated all findings in a Replication subsample from the same cohort. Multiple sensitivity and robustness analyses verified consistency of our findings.

MATERIALS AND METHODS

Participants

We considered data from 11,875 children from the ABCD 2.0.1 release. The data were collected on 21 sites across the United States (https://abcdstudy.org/contact/), and aimed to be representative of the sociodemographic diversity of the US population of 9-10 year old children (Garavan et al., 2018). To ensure that the study had enough statistical power to characterize a large variety of developmental trajectories, the ABCD study aimed for 50% of their sample to exhibit early signs of internalizing/externalizing symptoms (Garavan et al., 2018). Ethical review and approval of the protocol was obtained from the Institutional Review Board (IRB) at the University of California, San Diego, as well as from local IRB (Auchter et al., 2018). Parents/guardians and children provided written assent (Clark et al., 2018). After excluding participants with incomplete structural MRI, resting-state functional MRI (rs-fMRI), or behavioral data, MRI preprocessing and quality control, and after excluding sites with less than 20 participants, our main analyses included 5,251 unrelated children (2,577 female (49%), 9.94 ± 0.62 years old, 19 sites). We divided this sample into Discovery (N=3,504, *i.e.,* 2/3 of the dataset) and Replication (N=1,747 *i.e.,* 1/3 of the dataset) subsamples, using randomized data partitioning with both subsamples being matched on age, sex, ethnicity, acquisition site, and overall psychopathology (*i.e.,* scores of the first principal component derived from the 118 items of the Achenbach Child Behavior Checklist (CBCL) (Achenbach and Rescorla, 2013). **Figure 1d** shows the distribution of these measures in the two samples.

Behavioral assessment

The parent-reported CBCL (Achenbach and Rescorla, 2013) is comprised of 119 items that measure various symptoms in the child's behavior in the past six months. Symptoms are rated on a three-point scale from (0=not true, 1=somewhat or sometimes true, 2=very true or always true). We used 118/119 items (see **Table S1** for a complete list of items); one item was removed ("Smokes, chews, or sniffs tobacco") as all participants from the discovery sample scored "0" for this question. In the replication sample, another item ("Uses drugs for nonmedical purposes - don't include alcohol or tobacco") was removed for the same reason. Effects of age, age^2, sex, site, and ethnicity were regressed out from the behavioral and imaging data prior to the PLS analysis to ensure that the LCs would not be driven by possible confounders (Kebets et al., 2021, 2019; Xia et al., 2018).

MRI acquisition and processing

Images were acquired across 21 sites in the United States with harmonized imaging protocols for GE, Philips, and Siemens scanners (Casey et al., 2018). The imaging acquisition protocol consisted of a localizer, T1-weighted images, 2 runs of rs-fMRI, diffusion-weighted images, T2-weighted images, 1-2 more runs of rs-fMRI, and the three task-fMRI acquisitions. See **Supplementary Methods** for details.

Minimally preprocessed T1-weighted, fMRI, and diffusion MRI data were used (Hagler et al., 2019). T1-weighted images were further processed using FreeSurfer 5.3.0 (Dale et al., 1999; Fischl et al., 1999a, 1999b; Ségonne et al., 2007, 2004). Functional images were aligned to the T1 images using boundary-based registration, followed by motion filtering, nuisance regression, global signal regression, censoring and bandpass filtering. Finally, preprocessed time series were projected onto FreeSurfer fsaverage6 surface space and smoothed using a 6 mm full-width half maximum kernel. The same processing was applied to task-fMRI data. We used the processed diffusion MRI data, which included diffusion tensor metrics in 35 major white matter tracts (Hagler Jr et al., 2009). See **Supplementary Methods** for details.

Extraction of functional and structural features

Resting-state functional connectivity (RSFC) was computed as the Pearson's correlation between the average timeseries among 400 cortical (Schaefer et al., 2018) and 19 subcortical (Fischl et al., 2002) regions (**Figure 1a**), yielding 87,571 connections for each participant. Censored frames were not considered when computing FC. Age, age^2, sex, site, ethnicity, head motion (mean framewise displacement [FD]), and image intensity (mean voxel-wise differentiated signal variance [DVARS]) were further regressed out from the RSFC data.

Surface area, thickness and volume were extracted from the same 400 cortical regions (Schaefer et al., 2018). Age, age^2, sex, site, and ethnicity were also regressed out from each parcel-wise structural measure; cortical thickness and volume measures were additionally adjusted for total intracranial volume, and surface area additionally for total surface area.

To reduce data dimensionality before combining the different imaging modalities, we applied principal components analysis (PCA) over each feature (*i.e.,* surface area, cortical thickness, cortical volume, RSFC), and selected PCA scores of the number of components explaining 50% of the variance within each data modality, before concatenating them (see **Figure 1b**). The chosen 50% threshold sought to balance the relative contribution of modalities - to prevent the relatively larger number of RSFC features (compared to structural features) from

overpowering the analyses (see **Supplemental Methods** and **Figure S2**); however, we also report results for different thresholds (see Control analyses). We obtained 50, 58, 57, and 256 principal components for surface area, thickness, volume, and RSFC respectively, resulting in 421 components in total.

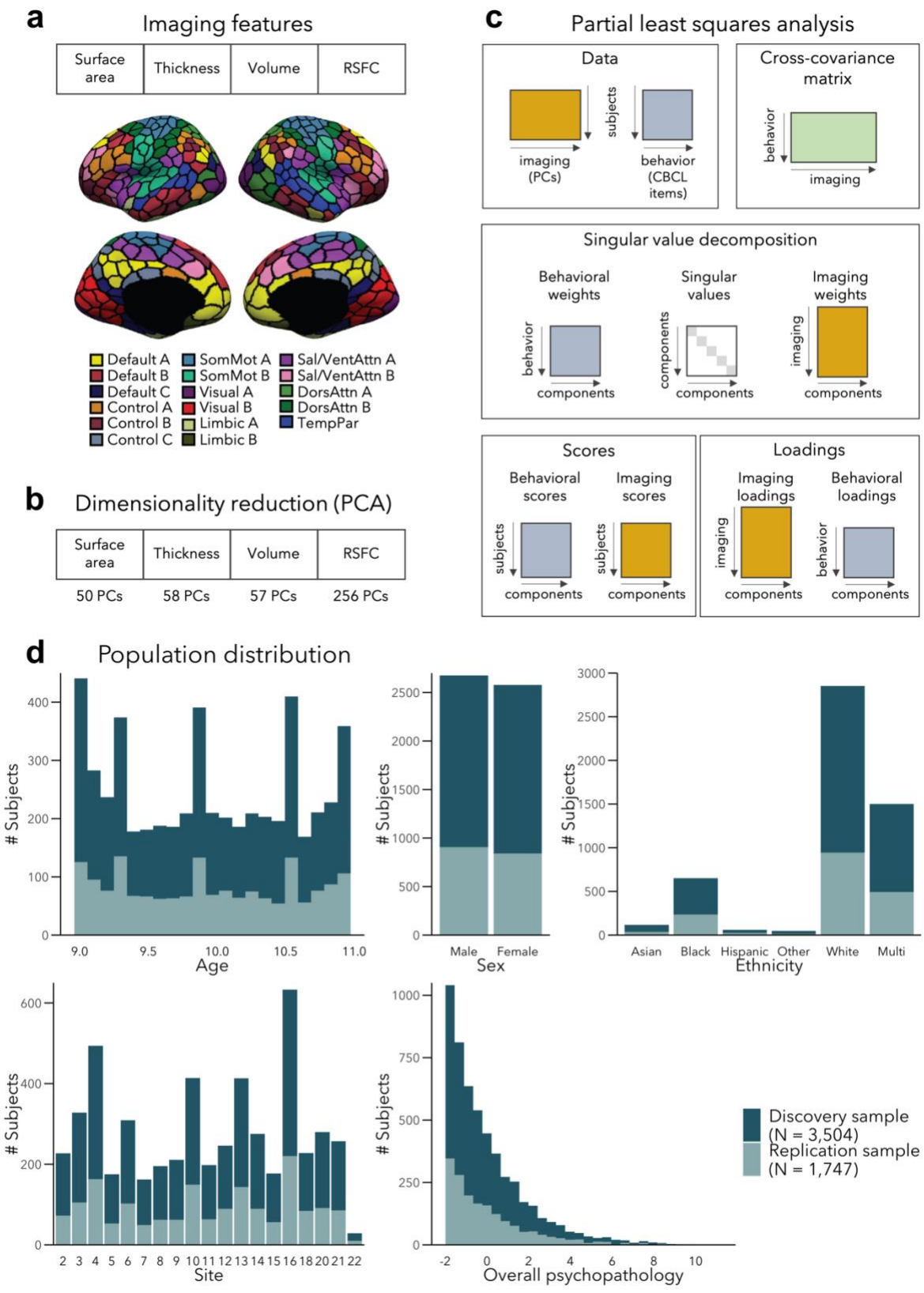

Figure 1. Analysis workflow **(a)** Imaging features **(b)** The imaging data underwent dimensionality reduction using principal components analysis (PCA), keeping the components explaining 50% of the variance within each imaging modality, resulting in 421 components in total. **(c)** Partial least squares analysis between the multimodal imaging data (421 PCs) and the behavioral data (118 CBCL items). **(d)** Distribution of age, sex, ethnicity, acquisition site, and overall psychopathology were matched between the discovery and replication samples.

Overall psychopathology represents the first principal component derived from all the CBCL items used in the main analysis.

Partial least squares analysis

Partial least squares (PLS) correlation analysis (McIntosh and Lobaugh, 2004; McIntosh and Mišić, 2013) was used to identify *latent components* (LCs) that optimally related children's symptoms (indexed by the CBCL) to structural and functional imaging features (**Figure 1c**). PLS maximizes the covariance between two data matrices by linearly projecting the behavioral and imaging data into a low-dimensional space. Briefly, a cross-covariance matrix was computed between imaging and behavioral data matrices. Singular value decomposition was applied to the cross-covariance matrix, resulting in three matrices: a diagonal matrix containing singular values, as well as imaging and behavioral *weights*. Participants' imaging and behavioral *composite scores* were computed by multiplying their original imaging and behavior data with their respective weights. The contribution of each variable to the LCs was determined by computing Pearson's correlations between participants' composite scores and their original data, which we refer to as *loadings*. The covariance explained by each LC was computed as the squared singular value divided by the squared sum of all singular values. Statistical significance of the LCs was assessed using permutation testing (10,000 permutations accounting for site) over the singular values of the first 5 LCs, while accounting for acquisition site (*i.e.,* data were permuted between participants from the same site). Loading stability was determined using bootstraps, whereby data were sampled 1,000 times with replacement among participants from the same site. Bootstrapped z-scores were computed by dividing each loading by its bootstrapped standard deviation. To limit the number of multiple comparisons, the bootstrapped rs- and task FC loadings were averaged across edge pairs within and between 18 networks, before computing z-scores. The procedure was performed in both the discovery and replication samples. See **Supplementary Methods** for more details.

Associations with cortical organization

To map psychopathology-related structural and functional abnormalities along the sensory-to-transmodal gradient of brain organization, we applied diffusion map embedding (Coifman et al., 2005), a nonlinear dimensionality reduction technique to the RSFC data. Essentially, strongly interconnected parcels will be closer together in this low dimensional embedding space (*i.e.,* have more similar scores), while parcels with little or no inter-covariance will be further apart (and have more dissimilar scores). Previous work has shown that spatial gradients of RSFC variations derived from nonlinear dimensionality reduction recapitulate the putative

cortical hierarchy (Bernhardt et al., 2022; Margulies et al., 2016; Mesulam, 1998), suggesting that functional gradients might approximate an inherent coordinate system of the human cortex. To derive the functional gradient, we calculated a cosine similarity matrix from the average RSFC matrix of our full sample (*i.e.,* discovery and replication samples together, N=5,251), using the top 10% entries for each row. The α parameter (set at $\alpha = 0.5$) controls the influence of the density of sampling points on the manifold ($\alpha = 0$, maximal influence; $\alpha = 1$, no influence), while the t parameter (set at $t = 0$) scales eigenvalues of the diffusion operator. These parameters were set to retain the global relations between data points in the embedded space, following prior applications (Hong et al., 2019; Margulies et al., 2016; Paquola et al., 2019). To facilitate comparison with previous work (Margulies et al., 2016), the connectivity gradient we derived from our ABCD sample was aligned to gradients derived from the Human Connectome Project (HCP) healthy young adult dataset, available in the BrainSpace toolbox (Vos de Wael et al., 2020), using Procrustes alignment. In a control analysis, we also computed connectivity gradients without aligning them to the HCP dataset to verify whether the gradients' order would change, as a recent study has shown that the principal gradient transitioned from the somatosensory/motor-to-visual to the sensory-to-transmodal gradient between childhood and adolescence (Dong et al., 2021). Finally, for gradient-based contextualization of our findings, we computed Pearson's correlations between cortical PLS loadings (within each imaging modality) and scores from the first gradient (*i.e.,* recapitulating the sensory-to-transmodal axis of cortical organization). Statistical significance of spatial associations was assessed using 1,000 spin tests that control for spatial autocorrelations (Alexander-Bloch et al., 2018), followed by FDR correction for multiple comparisons ($q < 0.05$).

Associations with task FC & diffusion imaging data

Task FC and diffusion tensor metrics were also explored in a *post hoc* association analyses in smaller subsamples. Following the same pipeline as for the rs-fMRI data, FC was computed across the entire timecourse of each fMRI task (thereby capturing both the active task and rest conditions), *i.e.*, the Monetary Incentive Delay (MID) task, which measures domains of reward processing, the Emotional N-back (EN-back) task, which evaluates memory and emotion processing, and the Stop Signal Task (SST), which engages impulsivity and impulse control. Details about task paradigms and conditions can be found elsewhere (Casey et al., 2018). After excluding subjects that did not pass both rs- and task fMRI quality control, MID and SST data were available in 2,039 participants, while EN-back data were available in 3,435 participants.

A total of 1,195 of participants overlapped across the three tasks and the discovery sample (39%). Task FC data were corrected for the same confounds as RSFC (*i.e.*, age, age^2, sex, site, ethnicity, mean FD, and mean DVARS). Diffusion tensor metrics included fractional anisotropy (FA) and mean diffusivity (MD) in 35 white matter tracts (Hagler Jr et al., 2009). FA measures directionally constrained diffusion of water molecules within the white matter and MD the overall diffusivity, and both metrics have been suggested to index fiber architecture and microstructure. Effects of age, age^2, sex, site, and ethnicity were regressed out from the FA and MD measures.

The contribution of task FC and diffusion MRI features was computing by correlating participants' task FC and diffusion MRI data with their imaging and behavior composite scores (from the main PLS analysis using structural and RSFC features). As for other modalities, the loadings' stability was determined via bootstraps (*i.e.*, 1,000 samples with replacement accounting for site).

Control analyses

Several analyses assessed reliability. First, we repeated the PLS analysis in the replication sample (N=1,747, *i.e.*, 1/3 of our sample), and tested the reliability of our findings by computing Pearson's correlations between the obtained behavior/imaging loadings with the original loadings. Second, we repeated the PLS analyses while keeping principal components explaining 10-90% of the variance within each imaging modality, and compared resulting loadings to those of our original model (which kept principal components explaining 50% of the variance) via Pearson's correlation between loadings. For imaging loadings, we computed correlations for each imaging modality, then averaged correlations across all imaging modalities. Third, we assessed the effects of age and sex differences on the LCs, by computing associations between participants' imaging/behavior composite scores and their age and sex, using either t-tests (for associations with sex) or Pearson's correlations (for associations with age). *Post hoc* tests were corrected for multiple comparisons using FDR correction ($q < 0.05$). See **Supplemental Results** for details.

Data and code availability

The ABCD data are publicly available via the NIMH Data Archive (NDA). Processed data from this study (including imaging features, PLS loadings and composite scores) have been uploaded to the NDA. Researchers with access to the ABCD data will be able to download the data here: <NDA_URL>. The preprocessing pipeline can be found at

https://github.com/ThomasYeoLab/CBIG/tree/master/stable_projects/preprocessing/CBIG_fMRI_Preproc2016. Preprocessing code specific to this study can be found here: https://github.com/ThomasYeoLab/ABCD_scripts. The code for analyses can be found here: (https://github.com/valkebets/multimodal_psychopathology_components).

RESULTS

Significant latent components

PLS analysis revealed five significant LCs (all p=0.001 after permuting the first five LCs 10,000 times, accounting for site and FDR) in the discovery sample. They explained 21%, 4%, 3%, 3%, 2% of covariance between the imaging and behavioral data, respectively (**Figure S1**). LC1, LC2, LC3, and LC5 recapitulated the dimensions previously reported (Michelini et al., 2019), *i.e.,* general psychopathology (**LC1**), internalizing vs. externalizing (**LC2**), neurodevelopmental (**LC3**), and detachment (**LC5**)(**Table S2**). For the remainder of this article, we focus on LC1-LC3, as they were strongly correlated to previously identified factors (see **Table S2** for details), and have been more thoroughly documented previously (Holmes et al., 2021; Michelini et al., 2019; Modabbernia et al., 2022), but LCs 4-5 are described in the **Supplemental Results**.

General psychopathology component (LC1)

LC1 (r=0.36, permuted p=0.001; **Figure 2a**) recapitulated a previously described *p* factor (Alnæs et al., 2018; Caspi et al., 2014; Elliott et al., 2018; Kaczkurkin et al., 2017; Kebets et al., 2019; Lahey et al., 2011; Romer et al., 2018; Shanmugan et al., 2016; Van Dam et al., 2017), and strongly correlated (r=0.64, p<0.001; **Table S2**) with the *p* factor derived from CBCL items by Michelini and colleagues (Michelini et al., 2019). All symptom items loaded positively on LC1 – which is expected given prior data showing that every prevalent mental disorder loads positively on the *p* factor (Lahey et al., 2012). The top behavioral loadings include being inattentive/distracted, impulsive behavior, mood changes, rule breaking, and arguing (**Figure 2b,** see **Table S3** for all behavior loadings). Greater (*i.e.,* worse) psychopathology was overall associated with mainly volume and thickness reductions, while the pattern of surface area associations was more mixed encompassing increases as well as decreases (**Figure 2c,** see **Figure S4** for uncorrected structural imaging loadings, and **Figure S5** for subcortical volume loadings). Interestingly, there was a strong spatial correspondence between volume and surface area loadings (r=0.79, p_{spin}<0.001), and between volume and thickness loadings (r=0.43, p_{spin}<0.001; **Table S4**). Greater psychopathology was also associated with patterns of large-scale network organization (Schaefer et al., 2018; Yeo et al., 2011), namely increased RSFC between the default and executive control, default, dorsal and ventral attention networks, and decreased RSFC between the two attention networks, between visual and default networks, and between control and attention networks (**Figure 2d**, see also

Figure S5 for a zoom on subcortical-cortical loadings, and **Figure S6** for uncorrected RSFC loadings). We also found significant spatial correspondence between within-network and between-network RSFC (r=-0.35, p_{spin}<0.001), and to a lesser extent between within-network RSFC and thickness (r=-0.13, p_{spin}=0.040), and between within-network RSFC and surface area (r=0.11, p_{spin}=0.048; **Table S4**).

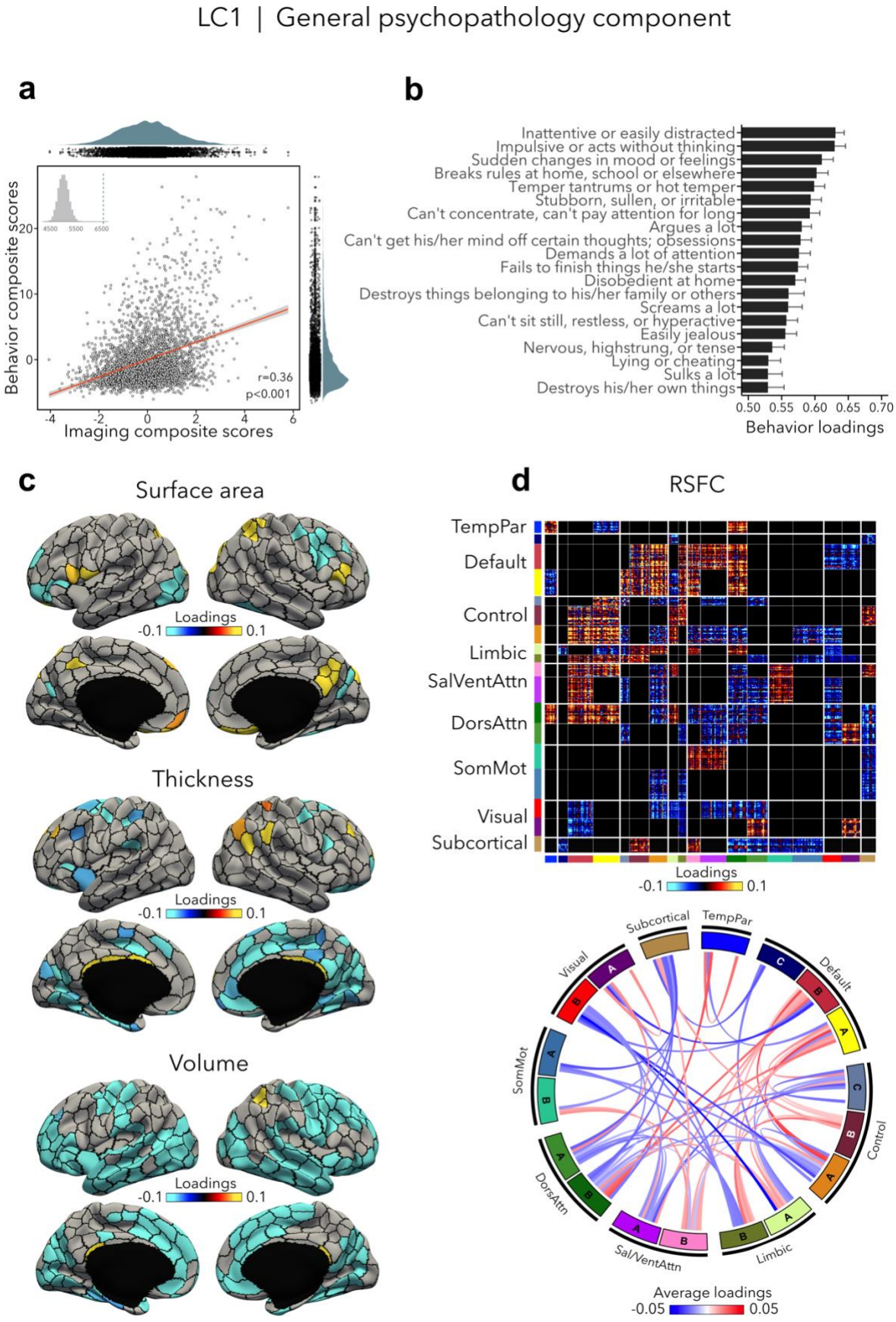

Figure 2. LC1 represents the general psychopathology (*p*) factor. **(a)** Correlation between imaging and behavior composite scores (r=0.36, permuted p=0.001). Each dot represents a different participant from the discovery sample. The inset on the top left shows the null distribution of (permuted) singular values from the permutation test, while the dotted line shows the original singular value. **(b)** Top behavior loadings characterizing this

component. Higher scores represent higher (*i.e.,* worse) symptom severity. Error bars indicate bootstrap-estimated confidence intervals. **(c)** Significant surface area, thickness, volume loadings (after bootstrap resampling and FDR correction q<0.05) associated with LC1. **(d)** Significant RSFC loadings (after bootstrap resampling and FDR correction q<0.05) associated with LC1. RSFC loadings were thresholded, whereby only within-network or between-network blocks with significant bootstrapped Z-scores are shown. Network blocks follow the colors associated with the 17 Yeo networks (Schaefer et al., 2018; Yeo et al., 2011) and subcortical regions (Fischl et al., 2002). Chord diagram summarizing significant within- and between-network RSFC loadings. See also **Figure 1a** for more detailed network visualization. DorsAttn, dorsal attention; RSFC, resting-state functional connectivity; SalVentAttn, salience/ventral attention; SomMot, somatosensory-motor; TempPar, temporoparietal.

Internalizing vs. externalizing component (LC2)

LC2 (r=0.34, permuted p=0.001; **Figure 3a**) contrasted internalizing *vs*. externalizing symptoms - two broad dimensions that are driven by covariation of symptoms among internalizing and externalizing disorders (Lahey et al., 2012, 2011). Here, higher (*i.e.*, positive) behavior loadings indicated increased internalizing symptoms, such as fear or anxiety, worrying, and feeling self-conscious, while lower (*i.e.,* negative) behavior loadings expressed increased externalizing symptoms, such as aggressivity and rule-breaking behaviors (**Figure 3b, Table S3**). At the brain level, greater internalizing symptoms were associated with widespread decreases in cortical thickness, and mixed patterns of increases and decreases in surface area and volume (**Figures 3c, S4-5**). There was a strong spatial correspondence between volume and surface area patterns (r=0.83, p_{spin}<0.001), and between volume and thickness loadings (r=0.53, p_{spin}<0.001; **Table S4**). In terms of brain organization, worse internalizing symptoms reflected lower RSFC within the somatomotor network and between the somatomotor and attention networks, and higher RSFC between the somatomotor network and the default and control networks (**Figures 3d, S5-6**). Again, there was a significant negative correlation between within-network RSFC and between-network RSFC (r=-0.42, p_{spin}<0.001; **Table S4**), but not between structural and functional loadings. Note that these brain patterns are inversely related to greater/worse externalizing symptoms, *e.g.*, increased thickness, higher RSFC within the somatomotor network.

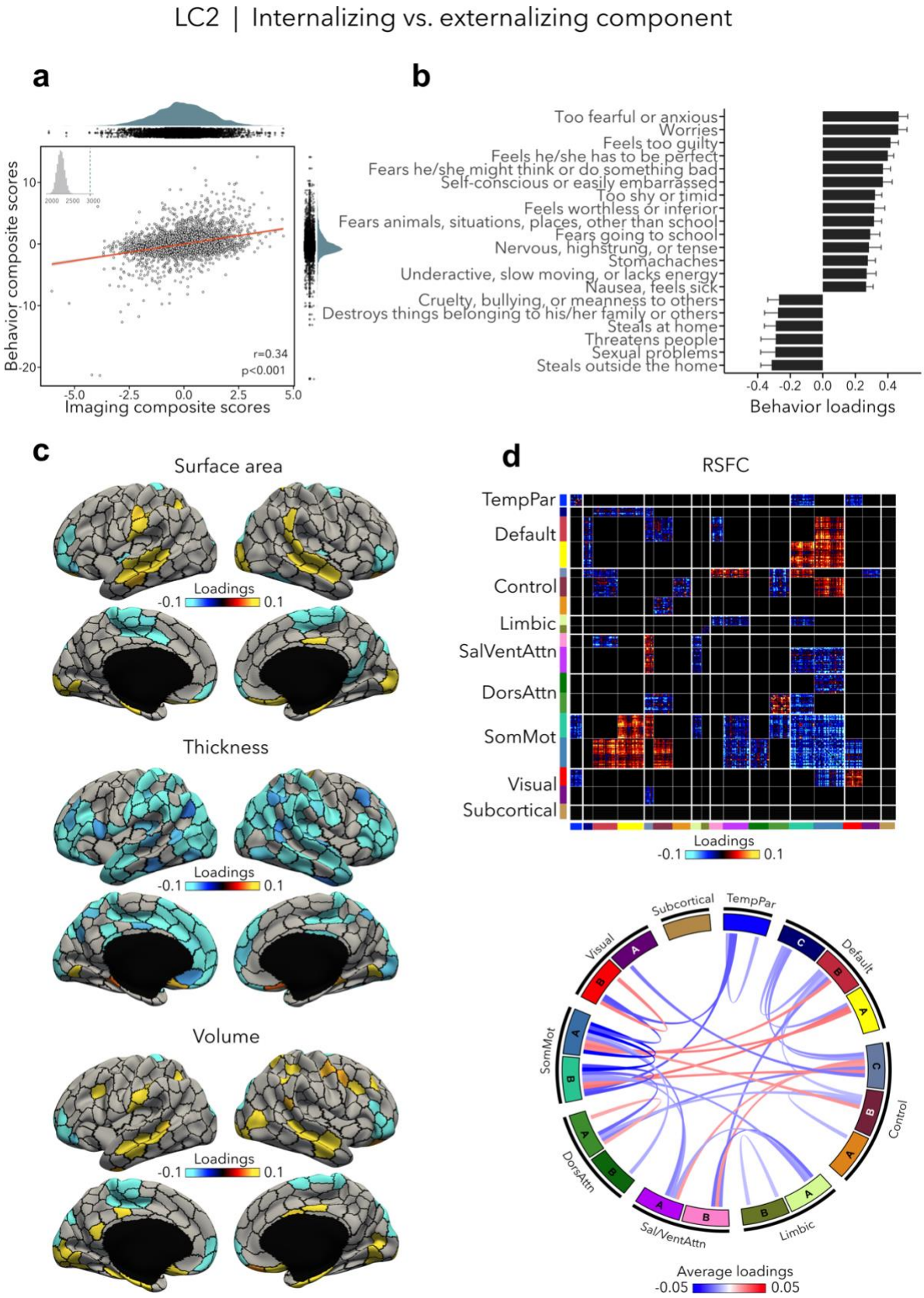

Figure 3. Internalizing vs. externalizing component (LC2). **(a)** Correlation between imaging and behavior composite scores (r=0.34, permuted p=0.001). Each dot represents a different participant from the discovery sample. The inset on the top left shows the null distribution of (permuted) singular values from the permutation test, while the dotted line shows the original singular value. **(b)** Top absolute behavior loadings characterizing this component. Higher loadings represent increased (*i.e.,* worse) internalizing symptoms, while lower loadings

represent worse externalizing symptoms. Error bars indicate bootstrap-estimated confidence intervals. **(c)** Significant surface area, thickness, volume loadings (after bootstrap resampling and FDR correction q<0.05) associated with LC2. **(d)** Significant RSFC loadings were thresholded, whereby only within-network or between-network blocks with significant bootstrapped Z-scores are shown. Network blocks following the colors associated with the 17 Yeo networks (Schaefer et al., 2018; Yeo et al., 2011) and subcortical regions (Fischl et al., 2002). Chord diagram summarizing significant within- and between-network RSFC loadings. See also **Figure 1a** for more detailed network visualization. DorsAttn, dorsal attention; RSFC, resting-state functional connectivity; SalVentAttn, salience/ventral attention; SomMot, somatosensory-motor; TempPar, temporoparietal.

Neurodevelopmental component (LC3)

LC3 (r=0.35, permuted p<0.001; **Figure 4a**) was driven by neurodevelopmental symptoms, such as concentration difficulties and inattention, daydreaming and restlessness (**Figure 4b, Table S3**), which were contrasted to a mix of symptoms characterized by emotion dysregulation. Greater neurodevelopmental symptoms were associated with increased surface area and volume in temporo-parietal regions and decreased surface area and volume in prefrontal as well as in occipital regions, but also with increased thickness in temporo-occipital areas and decreased thickness in prefrontal regions (**Figures 4c, S4-5**). Again, we found a strong spatial correspondence between volume and surface area loadings (r=0.92, p_{spin}<0.001), and between volume and thickness loadings (r=0.32, p_{spin}<0.001; **Table S4**). Worse neurodevelopmental symptomatology was also related to decreased RSFC within most cortical networks such as the default, control, dorsal and ventral attention, and somatomotor networks, and increased RSFC between control, default and limbic networks on the one side, and attention and somatomotor networks on the other side (**Figures 4d, S5-6**). Within-network RSFC and between-network RSFC were negatively correlated (r=-0.45, p_{spin}<0.001). Interestingly, there was also significant correspondence between thickness and between-network RSFC (r=0.28, p_{spin}=0.004), and between volume and between-network RSFC (r=0.21, p_{spin}=0.019; **Table S4**).

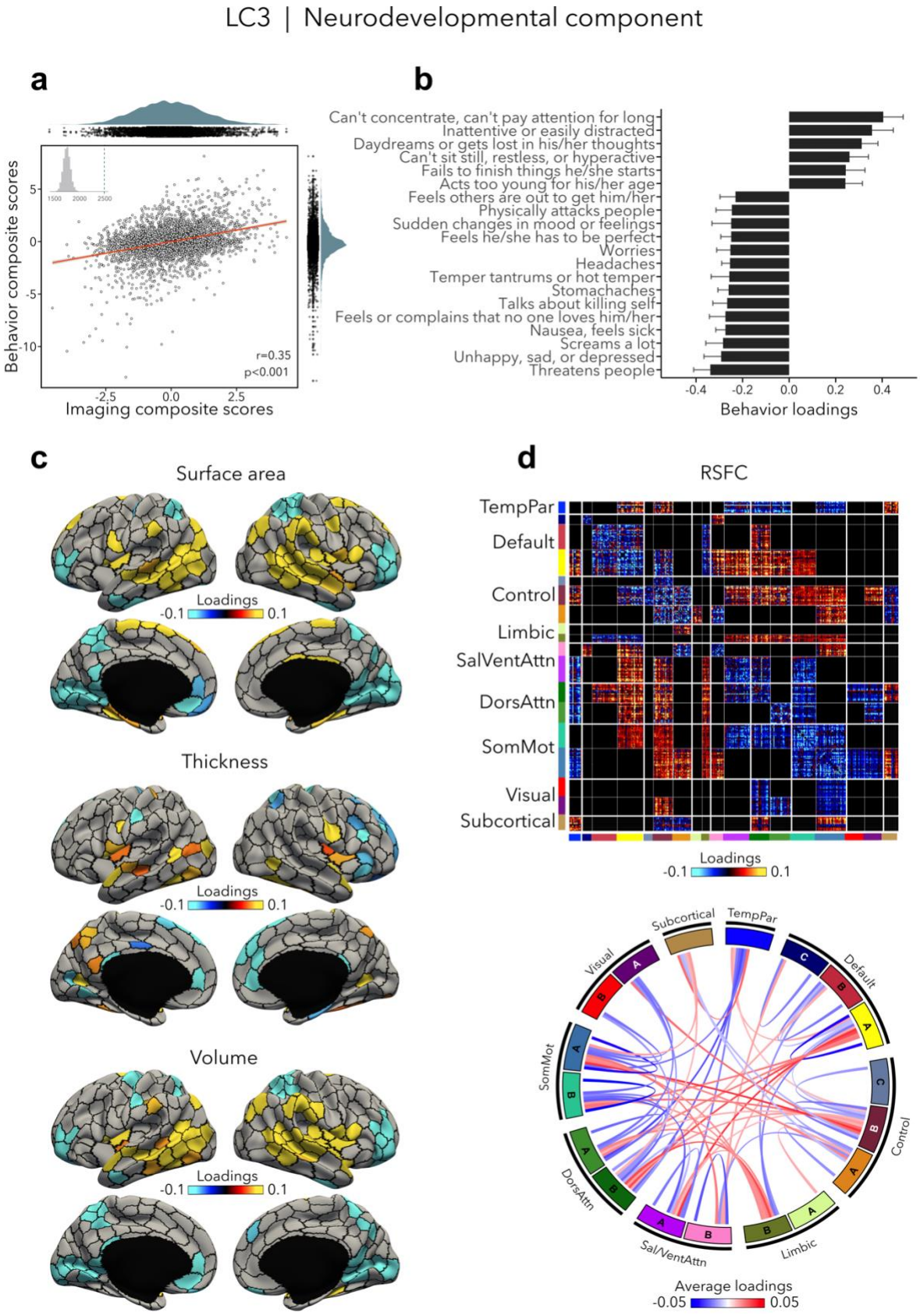

Figure 4. Neurodevelopmental component (LC3). **(a)** Correlation between imaging and behavior composite scores (r=0.35, permuted p=0.001). Each dot represents a different participant from the discovery sample. The inset on the top left shows the null distribution of (permuted) singular values from the permutation test, while the dotted line shows the original singular value. **(b)** Top absolute behavior loadings characterizing this component. Higher loadings represent increased (*i.e.,* worse) neurodevelopmental symptoms, while lower loadings represent

a mix of externalizing and internalizing symptoms. Error bars indicate bootstrap-estimated confidence intervals. **(c)** Significant surface area, thickness, volume loadings (after bootstrap resampling and FDR correction q<0.05) associated with LC3. **(d)** Significant RSFC loadings were thresholded, whereby only within-network or between-network blocks with significant bootstrapped Z-scores are shown. Network blocks following the colors associated with the 17 Yeo networks (Schaefer et al., 2018; Yeo et al., 2011) and subcortical regions (Fischl et al., 2002). Chord diagram summarizing significant within- and between-network RSFC loadings. See also **Figure 1a** for more detailed network visualization. DorsAttn, dorsal attention; RSFC, resting-state functional connectivity; SalVentAttn, salience/ventral attention; SomMot, somatosensory-motor; TempPar, temporoparietal.

Association with functional gradient

The primary functional gradient explained 28% of the RSFC variance, and differentiated primary somatosensory/motor and visual areas from transmodal association cortices (**Figure 5b**). These results replicate previous findings obtained with RSFC in a healthy adult cohort (Margulies et al., 2016). Since previous research had found that the sensory-to-transmodal gradient only becomes the 'principal' gradient around 12-13 years old (Dong et al., 2021), we also computed gradients without aligning it to the HCP gradient to verify whether the gradient order would change, but found the principal gradient to be virtually identical to its aligned counterpart (**Figure S3**). We note that the second gradient (contrasting somatosensory/motor and visual areas) explained almost the same amount of variance as the first gradient (*i.e.*, 26%, see **Figure 5a**), which may suggest that participants in our sample have only recently transitioned towards a more mature functional organization, *i.e.*, more spatially distributed (Dong et al., 2021). Next, we tested whether imaging loadings associated to the LCs would follow this sensory-to-transmodal axis (Sydnor et al., 2021) by assessing spatial correspondence while adjusting for spatial autocorrelations via spin permutation tests (Alexander-Bloch et al., 2018)(see **Table S5**). Between-network RSFC loadings for LC1 and LC3 showed a strong positive correlation to the principal gradient (LC1: r=0.43, p_{spin}<0.001; LC3: r=0.33, p_{spin}<0.001; **Figure 5d**), *i.e.*, between-network connectivity was higher in transmodal regions and lower in sensory areas. Within-network RSFC loadings for LC1, LC2 and LC3 also showed a significant albeit weak correlation with the sensory-to-transmodal gradient (LC1: r=-0.14, p_{spin}=0.010; LC2: (r=0.13, p_{spin}=0.032; LC3: r=0.17, p_{spin}=0.017; **Figure 5d**), *i.e.*, within-network FC was higher in sensory regions in LC1, and in higher-order regions in LCs 2-3. None of the structural loadings were associated with principal gradient scores.

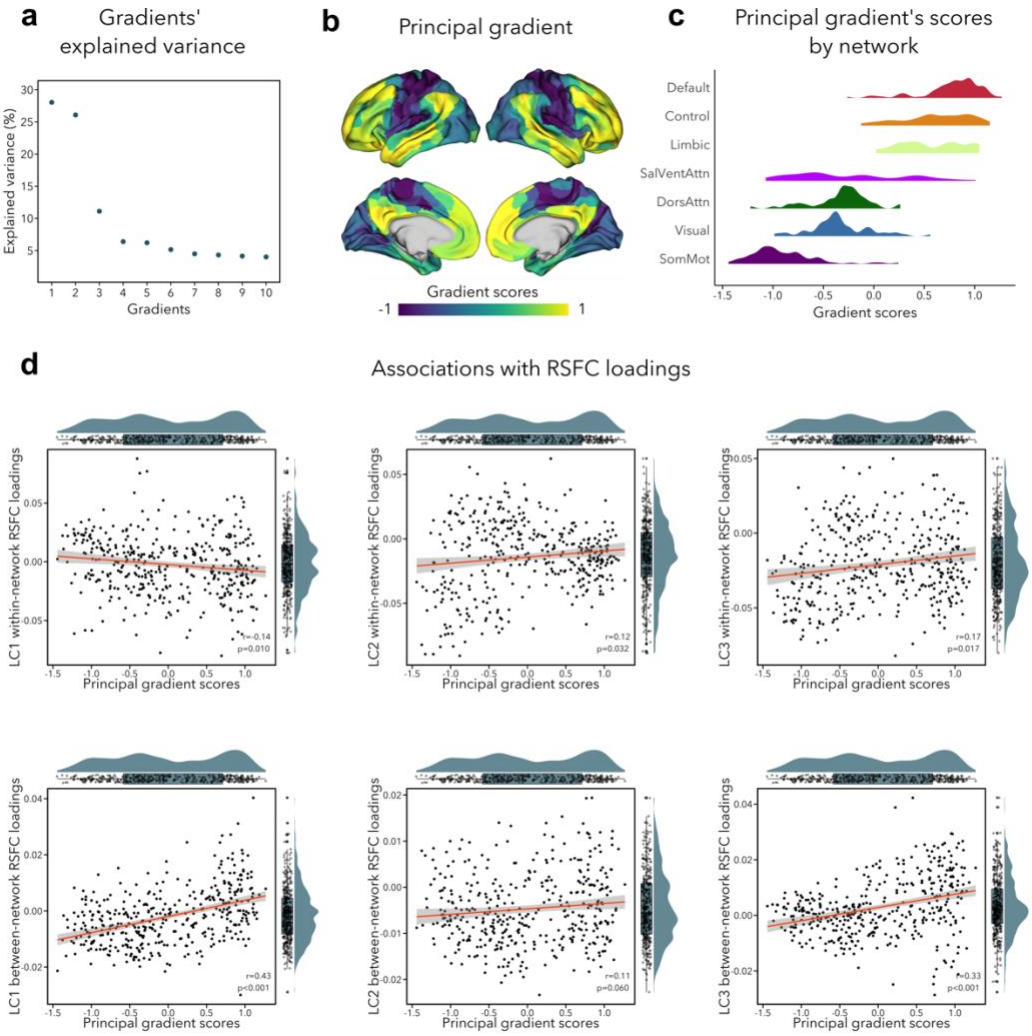

Figure 5. (a) Percentage of RSFC variance explained by each gradient **(b)** Principal functional gradient, anchored by transmodal association cortices on one end and by sensory regions on the other end. **(c)** Distribution of principal gradient's scores by cortical network (Yeo et al., 2011) **(d)** Associations between principal gradient scores and both within- and between-network RSFC loadings.

Contextualization w-r-t white matter architecture and across cognitive states

Our final analysis contextualized our findings with regards to white matter architecture and assessed the stability of functional organization across three cognitive states including reward, (emotional) working memory, and impulsivity (**Figure 6,** also see **Figure S6** for uncorrected task FC patterns). Greater psychopathology (LC1) was related to widespread decrease in FA and MD in all white matter tracts (see **Table S6** for diffusion-based loadings and z-scores for all white matter tracts). Higher internalizing and lower externalizing symptoms (LC2) were associated to higher FA within the left superior corticostriate-frontal and corticostriate tracts, and higher MD within the forceps major and parahippocampal cingulum. Finally, greater

neurodevelopmental symptoms (LC3) were related to decreased FA within the right cingulate cingulum, and within the left superior, temporal and parietal longitudinal fasciculus.

Regarding task FC organization, many patterns appeared to mirror those seen during rest. Greater psychopathology was associated with higher FC between control and default network across all states, including rest (**Figure 6c**). LC1 was also related to higher FC between sensory and attention networks during the EN-back task, and decreased FC between control and attention networks during MID and SST tasks. LC2 was related to decreased FC within the default network and between the default and control networks across all states, increased FC between somatomotor and control networks during MID and EN-back tasks, and between somatomotor and default network during EN-back and SST tasks. Finally, task FC patterns related to LC3 were similar to those observed during rest, *e.g.*, decreased within-network FC and higher FC between default and attention networks.

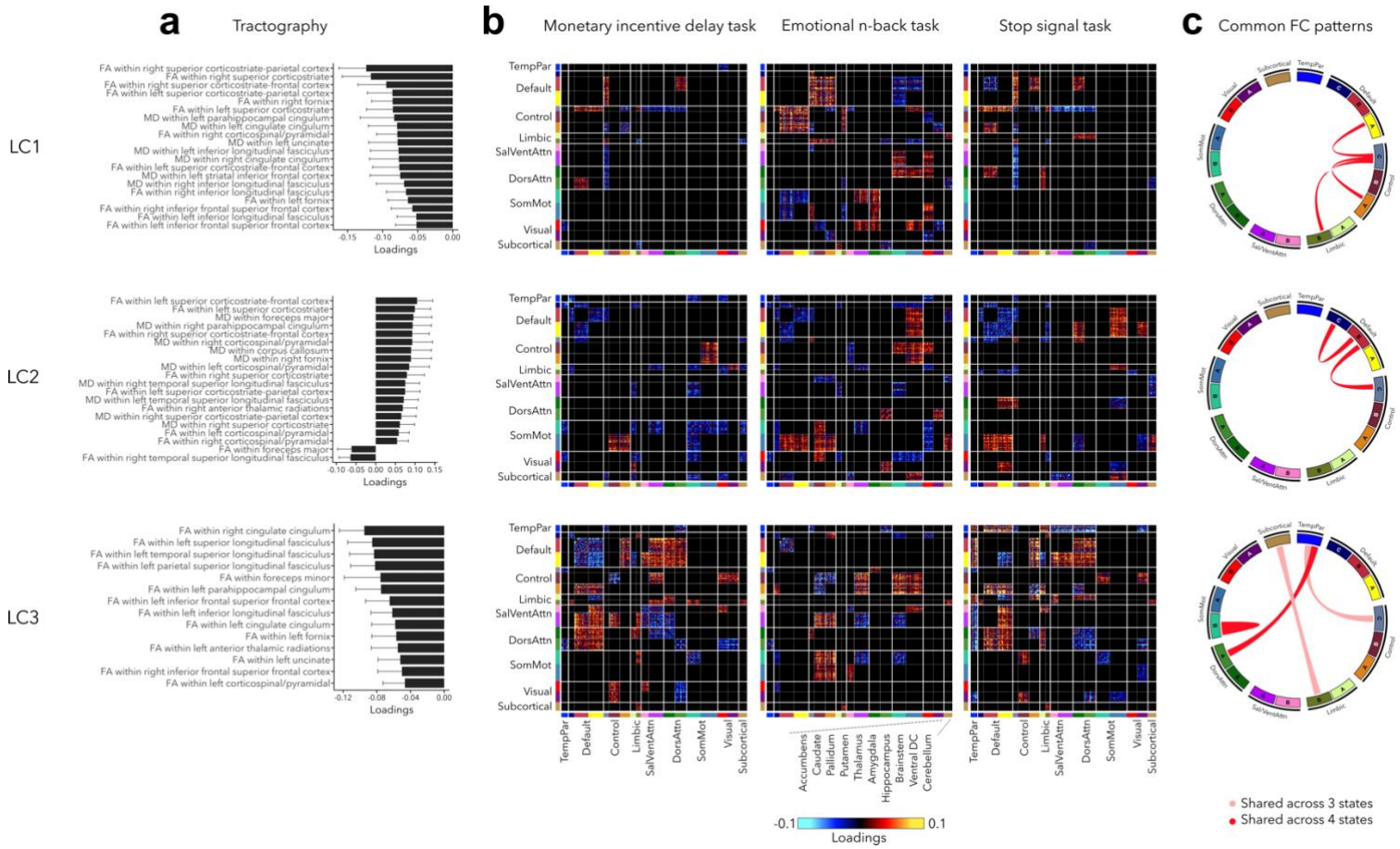

Figure 6. Significant diffusion MRI tractography loadings and task FC loadings associated with LC1-LC3, derived in smaller subsamples (N=3,275 for tractography and N=1,195 for task FC). **(a)** Error bars on the bar charts depicting tractography loadings on the right indicate bootstrap-estimated confidence intervals. **(b)** Task FC loadings were thresholded, whereby only within-network or between-network blocks with significant bootstrapped Z-scores are shown. Network blocks follow the colors associated with the 17 Yeo networks

(Schaefer et al., 2018; Yeo et al., 2011) and subcortical regions (Fischl et al., 2002). **(c)** FC patterns shared across either all 3 task states or all 4 states including rest. DorsAttn, dorsal attention; RSFC, resting-state functional connectivity; SalVentAttn, salience/ventral attention; SomMot, somatosensory-motor; TempPar, temporoparietal; Ventral FC, ventral diencephalon.

Generalizability and control analyses

Most main findings were validated in the replication sample (see **Figure 7**). First, we observed significant correlations between behavioral loadings of LC1-L4 in the discovery and replication samples (r=0.60-0.97). Behavior loadings for LC5 were also replicated with significance, but the correlation was lower (r=0.28, p=0.002). In terms of imaging loadings, RSFC loadings were replicated in LC1-LC5 (r=0.11-0.44, p<0.05); thickness loadings were replicated in LC1-LC4 (r=0.23-0.67, p_{spin}<0.05) but not LC5 (r=-0.23, p_{spin}=0.054) ; volume loadings were replicated in LC1, LC2, LC4, LC5 (r=0.16-0.35, p_{spin}<0.05) but not LC3 (r=0.02, p=0.446); finally, surface area loadings were only replicated in LC4 (r=0.23, p_{spin}=0.006). Second, we repeated our analyses while keeping principal components that explained 10%, 30%, 70% and 90% of variance in each imaging modality (instead of 50% as for the main analysis). Both behavior and imaging loadings were very similar to those in our main analysis, though we note that similarity was lower in the control analysis that kept principal components explaining 10% of the data (*i.e.,* 14 principal components), and for LC5 loadings (see **Supplementary Results** and **Table S7).** Third, we explored associations between age and sex, and psychopathology dimensions (see **Supplementary Results**). Notably, we found that male participants had higher composite scores on LC1 (*p* factor) and LC3 (neurodevelopmental symptoms), while female participants had higher composite scores on LC2 (internalizing symptoms).

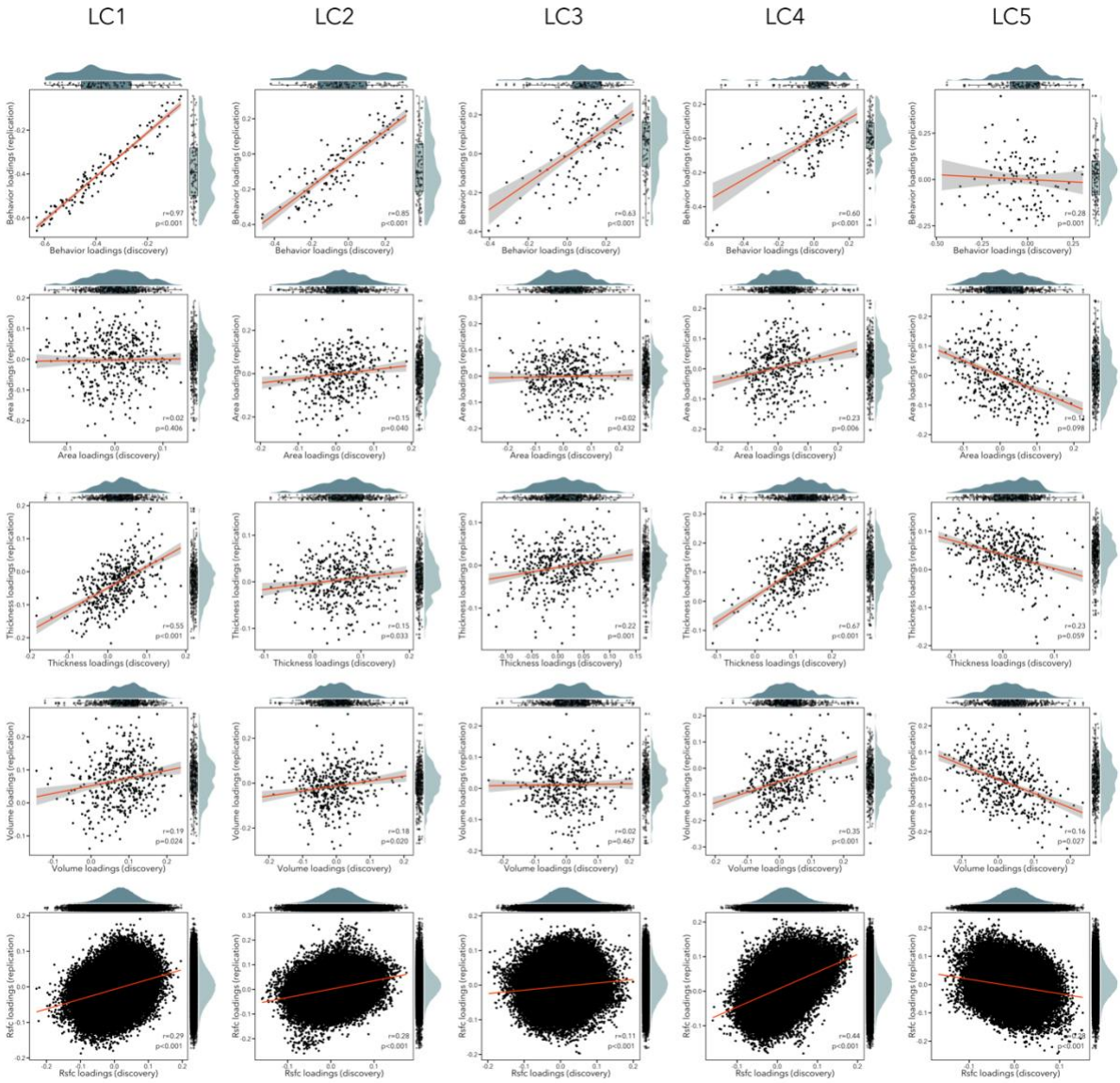

Figure 7. Scatterplots showing correlation between loadings in the discovery and replication sample for each modality (rows) and each LC (columns). The distribution of the loadings in the discovery sample are shown on the top x axis, while the distribution of the loadings in the replication sample are depicted on the right y axis.

DISCUSSION

The multitude of changes during typical and atypical neurodevelopment, and especially those occurring in late childhood and early adolescence, are complex and advocate for multidimensional approaches to comprehensively characterize risk patterns associated with developing mental illness. In the present work, we simultaneously delineated latent dimensions of psychopathology and their structural and functional neural substrates based on a large community-based developmental dataset, the ABCD cohort (Casey et al., 2018). Our findings mirrored the psychopathological hierarchy – starting with the *p* factor, followed by decreasingly broad dimensions - suggesting that this hierarchy is represented in multimodal cortical reorganization during development. The *p* factor, internalizing, externalizing, and neurodevelopmental dimensions were each associated to distinct morphological and intrinsic functional connectivity signatures. Latent components were also found to scale with initially held out neuroimaging features, including task-based connectivity patterns as well as diffusion MRI metrics sensitive to white matter architecture. Notably, connectivity signatures associated to the different components followed a recently described sensory-to-transmodal axis of cortical organization, which has been suggested to not only relate to the emergence of complex cognition and behavior, but also to the potential for neuroplasticity across the cortical landscape as well as risk for psychopathology (Sydnor et al., 2021). Finally, our findings were validated in a replication sample and were robust to several parameter variations in analysis methodology, supporting generalizability and consistency of our results.

Our study combined multiple measures tapping on brain structure that represent biologically meaningful phenotypes capturing distinct evolutionary, genetic, and cellular processes (Raznahan et al., 2011). These processes are closely intertwined, and follow a nonlinear (*i.e.*, a curvilinear inverted-U) trajectory during neurodevelopment that peak in late childhood/ adolescence (Raznahan et al., 2011) – but how and when these processes are disturbed by psychopathology is still poorly understood. We integrated structural neuroimaging features with measures of functional organization at rest, and sought to optimize their covariance with various symptom combinations, extending previous work that operated either on symptomatology (Michelini et al., 2019) or neuroimaging features alone (Elliott et al., 2018; Kebets et al., 2019; Romer et al., 2020; Shanmugan et al., 2016; Xia et al., 2018). Our integrated approach nevertheless replicated the dimensions found by Michelini and colleagues (Michelini et al., 2019), thereby extending them to a wide range of neurobiological substrates.

Moreover, our findings recapitulated the hierarchy within psychopathology (Kotov et al., 2017; Lahey et al., 2017), with the *p* factor explaining the highest covariance across multiple imaging features, and distinct structural and functional signatures related to internalizing, externalizing and neurodevelopmental dimensions. Previous research had found that disentangling the variation due to the *p* factor from other dimensions could be challenging, with sometimes few morphological or connectivity changes related to second-order dimensions left after adjusting for the *p* factor (*e.g.*, (Cui et al., 2021; Parkes et al., 2021)). By using PLS, which derives orthogonal components (McIntosh and Lobaugh, 2004; McIntosh and Mišić, 2013), we ensured that the neural substrates associated with LCs 2-5 were independent from those associated with the *p* factor (*i.e.*, LC1). Furthermore, we observed that structural patterns associated with psychopathology dimensions were highly similar across structural modalities, and somewhat similar to functional patterns though to a much lesser extent, which further suggests that structural and functional modalities provide complementary information to characterize vulnerability to psychopathology.

The *p* factor was associated with widespread decreases in cortical thickness, volume, but also in FA and MD, a pattern that likely reflects a general effect of decreased morphology associated with worse overall functioning, in line with previous research (Kaczkurkin et al., 2019; Romer et al., 2020). At the functional level, increased FC between control and default networks was found across all cognitive states – a pattern of dysconnectivity that had previously been reported across dimensions of mood, psychosis, fear, and externalizing behavior (Xia et al., 2018). Internalizing and externalizing symptoms were associated with mixed imaging patterns, due to these dimensions being contrasted in a single component characterized by both positive and negative behavior loadings. Cortical thickness patterns were consistent with a recent study reporting increased frontotemporal thickness associated with externalizing behavior in the same cohort (Modabbernia et al., 2022). These three broad dimensions (*i.e.*, *p* factor, internalizing, externalizing) are thought to be underpinned by sets of pleiotropic genetic influences that characterize the principal modes of genetic risk transmission for most disorders in childhood and adolescence (Pettersson et al., 2016, 2013), as well as by environmental events and contextual factors, such as familial situation, trauma, and broader socio-economic challenges, which may collectively modulate the way these disorders are expressed (Gur et al., 2019). The third component resembled the neurodevelopmental dimension, which captures inattention and autistic traits, and has previously been linked to intelligence and academic achievement (Kim et al., 2018; Michelini et al., 2021, 2019), and more generally a predictor of

learning (Holmes et al., 2021). At the functional level, the neurodevelopmental component was characterized by decreased within-network RSFC patterns across all cognitive states, in line with previous finding in the same cohort reporting lower RSFC within the default mode network, and altered connectivity of the default and control networks in association with neurodevelopmental symptoms (Karcher et al., 2021). Our findings add evidence to this cluster of symptoms having common neurobiological substrates that are distinct from other psychiatric disorders (Lee et al., 2019; Opel et al., 2020), which is in line with the known broad genetic overlap between neurodevelopmental symptoms, including autistic and ADHD behaviors, as well as learning difficulties, both throughout the general population and at the quantitative extreme (Pettersson et al., 2013; Ronald et al., 2008). There is also significant phenotypic overlap in the general population between autistic traits and ADHD symptoms, a co-occurrence that might be due to the disruptions in brain development during critical stages in gestation, infancy or early childhood, which could in turn lead to problems that would affect the normal growth process in areas such as learning, social interaction and behavioral control – a process that is primarily genetic in origin (Ronald et al., 2008). A recent study found that polygenic risk scores for ADHD and autism were associated with the neurodevelopmental factor in the ABCD cohort, although the latter did not survive after adjusting for the *p* factor (Waszczuk et al., 2021).

Conceptual and analytic advances have begun to characterize cortical organization along gradual dimensions, offering a continuous description of cortical arealization and modularity (Bernhardt et al., 2022; Huntenburg et al., 2018). One major dimension situates large-scale networks along a spectrum running from unimodal regions supporting action and perception to heteromodal association areas implicated in abstract cognition (Margulies et al., 2016; Paquola et al., 2019). This core axis has been shown at the level of functional connectivity (Margulies et al., 2016), but also microarchitectural indices related to cortical myelination (Burt et al., 2018; Huntenburg et al., 2017; Paquola et al., 2019), cytoarchitecture (Goulas et al., 2018; Paquola et al., 2020, 2019), or gene expression (Burt et al., 2018). Strikingly, neurodevelopmental changes in the formation and maturation of large-scale networks have been found to follow a similar axis; moreover, there is the emerging view that this framework may offer key insights on the development of psychopathology (Sydnor et al., 2021), and in particular the increased vulnerability of transmodal association cortices in late childhood and early adolescence, as these systems are also found to undergo prolonged maturation and potential for plastic reconfigurations (Paquola et al., 2019; Park et al., 2022b). Indeed, the

default network progressively becomes more integrated (among distant regions) and more regionally segregated (locally) between middle childhood to early adolescence, paralleling increasing abstract and logical thinking. This fine-tuning is underpinned by a gradual differentiation between higher-order and lower-order regions, which may be dependent on the maturation of association cortices. As they subserve cognitive, mentalizing and socioemotional processes, their maturational variability is thought to underpin inter-individual variability in psychosocial functioning and mental illness (Sydnor et al., 2021). We found that between-network RSFC loadings related to the *p* factor followed the sensory-to-transmodal gradient, with the default and control networks yielding higher between-network FC (*i.e.*, greater integration) while sensory systems exhibited lower between-network FC (*i.e.*, greater segregation), suggesting that connectivity between the two anchors of the principal gradient might be affected by the *p* factor. This finding is in line with recent studies showing that the sensory-to-transmodal axis is impacted across several disorders (Hettwer et al., 2022; Opel et al., 2020; Park et al., 2022a). As the *p* factor represents a general liability to all common forms of psychopathology, this points towards a disorder-general biomarker of dysconnectivity between lower-order and higher-order systems in the cortical hierarchy (Elliott et al., 2018; Kebets et al., 2019), which might be due to abnormal differentiation between higher-order and lower-order brain networks, possibly due to atypical maturation of higher-order networks. Interestingly, a similar pattern, albeit somewhat weaker, was also observed in association with the neurodevelopmental dimension. This suggests that neurodevelopmental difficulties might be related to alterations in various processes underpinned by sensory and association regions, in line with previous findings in autism showing a decreased differentiation between the two anchors of this gradient (Hong et al., 2019), mirroring impairment at both the sensory and higher-order level.

Our findings should be considered in light of some caveats. First, latent variable approaches such as PLS are powerful methods to characterize modes of covariation between multiple data sets, but they do not inform on any causal associations between them. Second, although they were validated in a replication cohort, verifying our findings in an independent dataset other than ABCD would indicate even broader generalizability. Furthermore, we only considered the ABCD cohort's baseline data in our analyses; longitudinal models assessing multiple time points will enable to further model developmental trajectories, test the stability of these dimensions over time, and how they relate to clinical phenotypes (Brieant et al., 2022; Leban, 2021). Our approach could be expanded to consider brain-environment interactions, as they

likely reinforce one another throughout development in shaping different forms of psychopathology (Sprooten et al., 2021). For instance, a recent study in the same cohort has shown that a broad range of environmental risk factors, including perinatal complications, socio-demographics, urbanization and pollution, characterized the main modes of variation in brain imaging phenotypes (Alnæs et al., 2020). Other factors have also been suggested to impact the development of psychopathology, such as executive functioning deficits, earlier pubertal timing, negative life events (Brieant et al., 2021), maternal depression, or psychological factors (*e.g.,* low effortful control, high neuroticism, negative affectivity). Finally, biases of caregiver reports have been shown with potential divergences between the child's and parent's report depending on family conflict (Shen et al., 2021). A large number of missing data in the teachers' reports prevented us from validating these brain-behavior associations with a second caretaker's report.

Despite these limitations, our study identified several dimensions of psychopathology which recapitulated the psychopathological hierarchy, alongside their structural and functional neural substrates. These findings are a first step towards capturing multimodal neurobiological changes underpinning broad dimensions of psychopathology, which might be used to predict future psychiatric diagnosis.

ACKNOWLEDGMENTS

VK acknowledges postdoctoral training support by the Transforming Autism Care Consortium (TACC) and the Montreal Neurological Institute (MNI). BTTY is currently supported by the Singapore National Research Foundation (NRF) Fellowship (Class of 2017), the NUS Yong Loo Lin School of Medicine (NUHSRO/2020/124/TMR/LOA), the Singapore National Medical Research Council (NMRC) LCG (OFLCG19May-0035), the NMRC STaR (STaR20nov-0003) and the USA NIH (R01MH120080). Any opinions, findings and conclusions or recommendations expressed in this material are those of the authors and do not reflect the views of the Singapore NRF or the Singapore NMRC. The computational work was partially performed using resources of the National Supercomputing Centre, Singapore (https://www.nscc.sg). BB acknowledges research support from the National Science and Engineering Research Council of Canada (NSERC Discovery-1304413), the CIHR (FDN-154298, PJT-174995), SickKids Foundation (NI17-039), Azrieli Center for Autism Research

(ACAR-TACC), BrainCanada, Healthy Brains and Healthy Lives, and the Tier-2 Canada Research Chairs program.

Data used in the preparation of this article were obtained from the Adolescent Brain Cognitive Development[SM] (ABCD) Study (https://abcdstudy.org), held in the NIMH Data Archive (NDA). This is a multisite, longitudinal study designed to recruit more than 10,000 children age 9-10 and follow them over 10 years into early adulthood. The ABCD Study® is supported by the National Institutes of Health and additional federal partners under award numbers U01DA041048, U01DA050989, U01DA051016, U01DA041022, U01DA051018, U01DA051037, U01DA050987, U01DA041174, U01DA041106, U01DA041117, U01DA041028, U01DA041134, U01DA050988, U01DA051039, U01DA041156, U01DA041025, U01DA041120, U01DA051038, U01DA041148, U01DA041093, U01DA041089, U24DA041123, U24DA041147. A full list of supporters is available at https://abcdstudy.org/federal-partners.html. A listing of participating sites and a complete listing of the study investigators can be found at https://abcdstudy.org/consortium_members/. ABCD consortium investigators designed and implemented the study and/or provided data but did not necessarily participate in the analysis or writing of this report. This manuscript reflects the views of the authors and may not reflect the opinions or views of the NIH or ABCD consortium investigators. The ABCD data repository grows and changes over time. The ABCD data used in this report came from http://dx.doi.org/10.15154/1504041.

Declarations of interest: None

REFERENCES

Abu-Akel, A., Allison, C., Baron-Cohen, S., Heinke, D., 2019. The distribution of autistic traits across the autism spectrum: evidence for discontinuous dimensional subpopulations underlying the autism continuum. Mol. Autism 10, 24. https://doi.org/10.1186/s13229-019-0275-3

Achenbach, T., Rescorla, L., 2013. Achenbach System of Empirically Based Assessment, in: Encyclopedia of Autism Spectrum Disorders. Springer New York, New York, NY, pp. 31–39.

Alexander-Bloch, A.F., Shou, H., Liu, S., Satterthwaite, T.D., Glahn, D.C., Shinohara, R.T., Vandekar, S.N., Raznahan, A., 2018. On testing for spatial correspondence between maps of human brain structure and function. NeuroImage 178, 540–551. https://doi.org/10.1016/j.neuroimage.2018.05.070

Alnæs, D., Kaufmann, T., Doan, N.T., Córdova-Palomera, A., Wang, Y., Bettella, F., Moberget, T., Andreassen, O.A., Westlye, L.T., 2018. Association of Heritable Cognitive Ability and Psychopathology With White Matter Properties in Children and Adolescents. JAMA Psychiatry 75, 287–295. https://doi.org/10.1001/jamapsychiatry.2017.4277

Alnæs, D., Kaufmann, T., Marquand, A.F., Smith, S.M., Westlye, L.T., 2020. Patterns of socio-cognitive stratification and perinatal risk in the child brain. https://doi.org/10.1101/839969

Astle, D.E., Holmes, J., Kievit, R., Gathercole, S.E., 2022. Annual Research Review: The transdiagnostic revolution in neurodevelopmental disorders. J. Child Psychol. Psychiatry 63, 397–417. https://doi.org/10.1111/jcpp.13481

Auchter, A.M., Hernandez Mejia, M., Heyser, C.J., Shilling, P.D., Jernigan, T.L., Brown, S.A., Tapert, S.F., Dowling, G.J., 2018. A description of the ABCD organizational structure and communication framework. Dev. Cogn. Neurosci., The Adolescent Brain Cognitive Development (ABCD) Consortium: Rationale, Aims, and Assessment Strategy 32, 8–15. https://doi.org/10.1016/j.dcn.2018.04.003

Baker, J.T., Dillon, D.G., Patrick, L.M., Roffman, J.L., Brady, R.O., Pizzagalli, D.A., Öngür, D., Holmes, A.J., 2019. Functional connectomics of affective and psychotic pathology. Proc. Natl. Acad. Sci. 116, 9050–9059. https://doi.org/10.1073/pnas.1820780116

Bernhardt, B.C., Smallwood, J., Keilholz, S., Margulies, D.S., 2022. Gradients in Brain Organization. NeuroImage 118987. https://doi.org/10.1016/j.neuroimage.2022.118987

Brieant, A., Ip, K.I., Holt-Gosselin, B., Gee, D., 2022. Parsing Heterogeneity in Developmental Trajectories of Internalizing and Externalizing Symptomatology in the Adolescent Brain Cognitive Development Study. https://doi.org/10.31234/osf.io/pz5s8

Brieant, A.E., Sisk, L.M., Gee, D.G., 2021. Associations among negative life events, changes in cortico-limbic connectivity, and psychopathology in the ABCD Study. Dev. Cogn. Neurosci. 52, 101022. https://doi.org/10.1016/j.dcn.2021.101022

Burt, J.B., Demirtaş, M., Eckner, W.J., Navejar, N.M., Ji, J.L., Martin, W.J., Bernacchia, A., Anticevic, A., Murray, J.D., 2018. Hierarchy of transcriptomic specialization across human cortex captured by structural neuroimaging topography. Nat. Neurosci. 21, 1251–1259. https://doi.org/10.1038/s41593-018-0195-0

Casey, B.J., Cannonier, T., Conley, M.I., Cohen, A.O., Barch, D.M., Heitzeg, M.M., Soules, M.E., Teslovich, T., Dellarco, D.V., Garavan, H., Orr, C.A., Wager, T.D., Banich, M.T., Speer, N.K., Sutherland, M.T., Riedel, M.C., Dick, A.S., Bjork, J.M., Thomas, K.M., Chaarani, B., Mejia, M.H., Hagler, D.J., Daniela Cornejo, M., Sicat, C.S., Harms, M.P., Dosenbach, N.U.F., Rosenberg, M., Earl, E., Bartsch, H., Watts, R., Polimeni, J.R., Kuperman, J.M., Fair, D.A., Dale, A.M., 2018. The Adolescent Brain Cognitive Development (ABCD) study: Imaging acquisition across 21 sites. Dev. Cogn. Neurosci. 32, 43–54. https://doi.org/10.1016/j.dcn.2018.03.001

Casey, B.J., Oliveri, M.E., Insel, T., 2014. A neurodevelopmental perspective on the research domain criteria (RDoC) framework. Biol. Psychiatry 76, 350–353. https://doi.org/10.1016/j.biopsych.2014.01.006

Caspi, A., Houts, R.M., Belsky, D.W., Goldman-Mellor, S.J., Harrington, H., Israel, S., Meier, M.H., Ramrakha, S., Shalev, I., Poulton, R., Moffitt, T.E., 2014. The p Factor: One General Psychopathology Factor in the Structure of Psychiatric Disorders? Clin. Psychol. Sci. J. Assoc. Psychol. Sci. 2, 119–137. https://doi.org/10.1177/2167702613497473

Cauda, F., Nani, A., Manuello, J., Premi, E., Palermo, S., Tatu, K., Duca, S., Fox, P.T., Costa, T., 2018. Brain structural alterations are distributed following functional, anatomic and genetic connectivity. Brain 141, 3211–3232. https://doi.org/10.1093/brain/awy252

Clark, D.B., Fisher, C.B., Bookheimer, S., Brown, S.A., Evans, J.H., Hopfer, C., Hudziak, J., Montoya, I., Murray, M., Pfefferbaum, A., Yurgelun-Todd, D., 2018. Biomedical ethics and clinical oversight in multisite observational neuroimaging studies with children and adolescents: The ABCD experience. Dev. Cogn. Neurosci., The Adolescent Brain Cognitive Development (ABCD) Consortium: Rationale, Aims, and Assessment Strategy 32, 143–154. https://doi.org/10.1016/j.dcn.2017.06.005

Coifman, R.R., Lafon, S., Lee, A.B., Maggioni, M., Nadler, B., Warner, F., Zucker, S.W., 2005. Geometric diffusions as a tool for harmonic analysis and structure definition of data: Diffusion maps. Proc. Natl. Acad. Sci. 102, 7426–7431. https://doi.org/10.1073/pnas.0500334102

Cui, Z., Pines, A.R., Larsen, B., Sydnor, V.J., Li, H., Adebimpe, A., Alexander-Bloch, A.F., Bassett, D.S., Bertolero, M., Calkins, M.E., Davatzikos, C., Fair, D.A., Gur, R.C., Gur, R.E., Moore, T.M., Shanmugan, S., Shinohara, R.T., Vogel, J.W., Xia, C.H., Fan, Y., Satterthwaite, T.D., 2021. Linking Individual Differences in Personalized Functional Network Topography to Psychopathology in Youth. https://doi.org/10.1101/2021.08.02.454763

Cuthbert, B.N., 2014. The RDoC framework: facilitating transition from ICD/DSM to dimensional approaches that integrate neuroscience and psychopathology. World Psychiatry 13, 28–35. https://doi.org/10.1002/wps.20087

Dale, A.M., Fischl, B., Sereno, M.I., 1999. Cortical surface-based analysis. I. Segmentation and surface reconstruction. NeuroImage 9, 179–194. https://doi.org/10.1006/nimg.1998.0395

de Lange, S.C., Scholtens, L.H., van den Berg, L.H., Boks, M.P., Bozzali, M., Cahn, W., Dannlowski, U., Durston, S., Geuze, E., van Haren, N.E.M., Hillegers, M.H.J., Koch, K., Jurado, M.Á., Mancini, M., Marqués-Iturria, I., Meinert, S., Ophoff, R.A., Reess, T.J., Repple, J., Kahn, R.S., van den Heuvel, M.P., 2019. Shared vulnerability for connectome alterations across psychiatric and neurological brain disorders. Nat. Hum. Behav. 3, 988–998. https://doi.org/10.1038/s41562-019-0659-6

Dong, H.-M., Margulies, D.S., Zuo, X.-N., Holmes, A.J., 2021. Shifting gradients of macroscale cortical organization mark the transition from childhood to adolescence. Proc. Natl. Acad. Sci. 118, e2024448118. https://doi.org/10.1073/pnas.2024448118

Elliott, M.L., Romer, A., Knodt, A.R., Hariri, A.R., 2018. A Connectome-wide Functional Signature of Transdiagnostic Risk for Mental Illness. Biol. Psychiatry 84, 452–459. https://doi.org/10.1016/j.biopsych.2018.03.012

Etkin, A., 2019. A Reckoning and Research Agenda for Neuroimaging in Psychiatry. Am. J. Psychiatry 176, 507–511. https://doi.org/10.1176/appi.ajp.2019.19050521

Fischl, B., Salat, D.H., Busa, E., Albert, M., Dieterich, M., Haselgrove, C., van der Kouwe, A., Killiany, R., Kennedy, D., Klaveness, S., Montillo, A., Makris, N., Rosen, B., Dale, A.M., 2002. Whole brain segmentation: automated labeling of neuroanatomical structures in the human brain. Neuron 33, 341–355.

Fischl, B., Sereno, M.I., Dale, A.M., 1999a. Cortical surface-based analysis. II: Inflation, flattening, and a surface-based coordinate system. NeuroImage 9, 195–207. https://doi.org/10.1006/nimg.1998.0396

Fischl, B., Sereno, M.I., Tootell, R.B., Dale, A.M., 1999b. High-resolution intersubject averaging and a coordinate system for the cortical surface. Hum. Brain Mapp. 8, 272–284.

Garavan, H., Bartsch, H., Conway, K., Decastro, A., Goldstein, R.Z., Heeringa, S., Jernigan, T., Potter, A., Thompson, W., Zahs, D., 2018. Recruiting the ABCD sample: Design considerations and procedures. Dev. Cogn. Neurosci., The Adolescent Brain Cognitive Development (ABCD) Consortium: Rationale, Aims, and Assessment Strategy 32, 16–22. https://doi.org/10.1016/j.dcn.2018.04.004

Goddings, A.-L., Mills, K.L., Clasen, L.S., Giedd, J.N., Viner, R.M., Blakemore, S.-J., 2014. The influence of puberty on subcortical brain development. NeuroImage 88, 242–251. https://doi.org/10.1016/j.neuroimage.2013.09.073

Goodkind, M., Eickhoff, S.B., Oathes, D.J., Jiang, Y., Chang, A., Jones-Hagata, L.B., Ortega, B.N., Zaiko, Y.V., Roach, E.L., Korgaonkar, M.S., Grieve, S.M., Galatzer-Levy, I., Fox, P.T., Etkin, A., 2015. Identification of a common neurobiological substrate for mental illness. JAMA Psychiatry 72, 305–315. https://doi.org/10.1001/jamapsychiatry.2014.2206

Goulas, A., Zilles, K., Hilgetag, C.C., 2018. Cortical Gradients and Laminar Projections in Mammals. Trends Neurosci. 41, 775–788. https://doi.org/10.1016/j.tins.2018.06.003

Gur, R.E., Moore, T.M., Rosen, A.F.G., Barzilay, R., Roalf, D.R., Calkins, M.E., Ruparel, K., Scott, J.C., Almasy, L., Satterthwaite, T.D., Shinohara, R.T., Gur, R.C., 2019. Burden of Environmental Adversity Associated With Psychopathology, Maturation, and Brain Behavior Parameters in Youths. JAMA Psychiatry 76, 966–975. https://doi.org/10.1001/jamapsychiatry.2019.0943

Hagler, D.J., Hatton, SeanN., Cornejo, M.D., Makowski, C., Fair, D.A., Dick, A.S., Sutherland, M.T., Casey, B.J., Barch, D.M., Harms, M.P., Watts, R., Bjork, J.M., Garavan, H.P., Hilmer, L., Pung, C.J., Sicat, C.S., Kuperman, J., Bartsch, H., Xue, F., Heitzeg, M.M., Laird, A.R., Trinh, T.T., Gonzalez, R., Tapert, S.F., Riedel, M.C., Squeglia, L.M., Hyde, L.W., Rosenberg, M.D., Earl, E.A., Howlett, K.D., Baker, F.C., Soules, M., Diaz, J., de Leon, O.R., Thompson, W.K., Neale, M.C., Herting, M., Sowell, E.R., Alvarez, R.P., Hawes, S.W., Sanchez, M., Bodurka, J., Breslin, F.J., Morris, A.S., Paulus, M.P., Simmons, W.K., Polimeni, J.R., van der Kouwe, A., Nencka, A.S., Gray, K.M., Pierpaoli, C., Matochik, J.A., Noronha, A., Aklin, W.M., Conway, K., Glantz, M., Hoffman, E., Little, R., Lopez, M., Pariyadath, V., Weiss, S.RB., Wolff-Hughes, D.L., DelCarmen-Wiggins, R., Feldstein Ewing, S.W., Miranda-Dominguez, O., Nagel, B.J., Perrone, A.J., Sturgeon, D.T., Goldstone, A., Pfefferbaum, A., Pohl, K.M., Prouty, D., Uban, K., Bookheimer, S.Y., Dapretto, M., Galvan, A., Bagot, K., Giedd, J., Infante, M.A., Jacobus, J., Patrick, K., Shilling, P.D., Desikan, R., Li, Y., Sugrue, L., Banich, M.T., Friedman, N., Hewitt, J.K., Hopfer, C., Sakai, J., Tanabe, J., Cottler, L.B., Nixon, S.J., Chang, L., Cloak, C., Ernst, T.,

Reeves, G., Kennedy, D.N., Heeringa, S., Peltier, S., Schulenberg, J., Sripada, C., Zucker, R.A., Iacono, W.G., Luciana, M., Calabro, F.J., Clark, D.B., Lewis, D.A., Luna, B., Schirda, C., Brima, T., Foxe, J.J., Freedman, E.G., Mruzek, D.W., Mason, M.J., Huber, R., McGlade, E., Prescot, A., Renshaw, P.F., Yurgelun-Todd, D.A., Allgaier, N.A., Dumas, J.A., Ivanova, M., Potter, A., Florsheim, P., Larson, C., Lisdahl, K., Charness, M.E., Fuemmeler, B., Hettema, J.M., Maes, H.H., Steinberg, J., Anokhin, A.P., Glaser, P., Heath, A.C., Madden, P.A., Baskin-Sommers, A., Constable, R.T., Grant, S.J., Dowling, G.J., Brown, S.A., Jernigan, T.L., Dale, A.M., 2019. Image processing and analysis methods for the Adolescent Brain Cognitive Development Study. NeuroImage 202, 116091. https://doi.org/10.1016/j.neuroimage.2019.116091

Hagler Jr, D.J., Ahmadi, M.E., Kuperman, J., Holland, D., McDonald, C.R., Halgren, E., Dale, A.M., 2009. Automated white-matter tractography using a probabilistic diffusion tensor atlas: Application to temporal lobe epilepsy. Hum. Brain Mapp. 30, 1535–1547.

Hettwer, M.D., Larivière, S., Park, B.Y., van den Heuvel, O.A., Schmaal, L., Andreassen, O.A., Ching, C.R.K., Hoogman, M., Buitelaar, J., van Rooij, D., Veltman, D.J., Stein, D.J., Franke, B., van Erp, T.G.M., Jahanshad, N., Thompson, P.M., Thomopoulos, S.I., Bethlehem, R. a. I., Bernhardt, B.C., Eickhoff, S.B., Valk, S.L., 2022. Coordinated cortical thickness alterations across six neurodevelopmental and psychiatric disorders. Nat. Commun. 13, 6851. https://doi.org/10.1038/s41467-022-34367-6

Holmes, J., Mareva, S., Bennett, M.P., Black, M., Guy, J., 2021. Higher-order dimensions of psychopathology in a neurodevelopmental transdiagnostic sample. J. Abnorm. Psychol. 130, 909–922. https://doi.org/10.1037/abn0000710

Hong, S.-J., Vos de Wael, R., Bethlehem, R.A.I., Lariviere, S., Paquola, C., Valk, S.L., Milham, M.P., Di Martino, A., Margulies, D.S., Smallwood, J., Bernhardt, B.C., 2019. Atypical functional connectome hierarchy in autism. Nat. Commun. 10, 1022. https://doi.org/10.1038/s41467-019-08944-1

Huntenburg, J.M., Bazin, P.-L., Goulas, A., Tardif, C.L., Villringer, A., Margulies, D.S., 2017. A Systematic Relationship Between Functional Connectivity and Intracortical Myelin in the Human Cerebral Cortex. Cereb. Cortex 27, 981–997. https://doi.org/10.1093/cercor/bhx030

Huntenburg, J.M., Bazin, P.-L., Margulies, D.S., 2018. Large-Scale Gradients in Human Cortical Organization. Trends Cogn. Sci. 22, 21–31. https://doi.org/10.1016/j.tics.2017.11.002

Insel, T., Cuthbert, B., Garvey, M., Heinssen, R., Pine, D.S., Quinn, K., Sanislow, C., Wang, P., 2010. Research domain criteria (RDoC): toward a new classification framework

for research on mental disorders. Am. J. Psychiatry 167, 748–751. https://doi.org/10.1176/appi.ajp.2010.09091379

Jernigan, T.L., Brown, T.T., Hagler, D.J., Akshoomoff, N., Bartsch, H., Newman, E., Thompson, W.K., Bloss, C.S., Murray, S.S., Schork, N., Kennedy, D.N., Kuperman, J.M., McCabe, C., Chung, Y., Libiger, O., Maddox, M., Casey, B.J., Chang, L., Ernst, T.M., Frazier, J.A., Gruen, J.R., Sowell, E.R., Kenet, T., Kaufmann, W.E., Mostofsky, S., Amaral, D.G., Dale, A.M., 2016. The Pediatric Imaging, Neurocognition, and Genetics (PING) Data Repository. NeuroImage, Sharing the wealth: Brain Imaging Repositories in 2015 124, 1149–1154. https://doi.org/10.1016/j.neuroimage.2015.04.057

Jones, J.S., the CALM Team, Astle, D.E., 2021. A Transdiagnostic Data-driven Study of Children's Behaviour and the Functional Connectome. Dev. Cogn. Neurosci. 101027. https://doi.org/10.1016/j.dcn.2021.101027

Kaczkurkin, A.N., Moore, T.M., Calkins, M.E., Ciric, R., Detre, J.A., Elliott, M.A., Foa, E.B., Garcia de la Garza, A., Roalf, D.R., Rosen, A., Ruparel, K., Shinohara, R.T., Xia, C.H., Wolf, D.H., Gur, R.E., Gur, R.C., Satterthwaite, T.D., 2017. Common and dissociable regional cerebral blood flow differences associate with dimensions of psychopathology across categorical diagnoses. Mol. Psychiatry. https://doi.org/10.1038/mp.2017.174

Kaczkurkin, A.N., Park, S.S., Sotiras, A., Moore, T.M., Calkins, M.E., Cieslak, M., Rosen, A.F.G., Ciric, R., Xia, C.H., Cui, Z., Sharma, A., Wolf, D.H., Ruparel, K., Pine, D.S., Shinohara, R.T., Roalf, D.R., Gur, R.C., Davatzikos, C., Gur, R.E., Satterthwaite, T.D., 2019. Evidence for Dissociable Linkage of Dimensions of Psychopathology to Brain Structure in Youths. Am. J. Psychiatry appiajp201918070835. https://doi.org/10.1176/appi.ajp.2019.18070835

Karcher, N.R., Michelini, G., Kotov, R., Barch, D.M., 2021. Associations Between Resting-State Functional Connectivity and a Hierarchical Dimensional Structure of Psychopathology in Middle Childhood. Biol. Psychiatry Cogn. Neurosci. Neuroimaging 6, 508–517. https://doi.org/10.1016/j.bpsc.2020.09.008

Kebets, V., Favre, P., Houenou, J., Polosan, M., Perroud, N., Aubry, J.-M., Van De Ville, D., Piguet, C., 2021. Fronto-limbic neural variability as a transdiagnostic correlate of emotion dysregulation. Transl. Psychiatry 11, 1–8. https://doi.org/10.1038/s41398-021-01666-3

Kebets, V., Holmes, A.J., Orban, C., Tang, S., Li, J., Sun, N., Kong, R., Poldrack, R.A., Yeo, B.T.T., 2019. Somatosensory-Motor Dysconnectivity Spans Multiple Transdiagnostic Dimensions of Psychopathology. Biol. Psychiatry.

Kim, S.H., Bal, V.H., Lord, C., 2018. Longitudinal follow-up of academic achievement in children with autism from age 2 to 18. J. Child Psychol. Psychiatry 59, 258–267. https://doi.org/10.1111/jcpp.12808

Kotov, R., Krueger, R.F., Watson, D., Achenbach, T.M., Althoff, R.R., Bagby, R.M., Brown, T.A., Carpenter, W.T., Caspi, A., Clark, L.A., Eaton, N.R., Forbes, M.K., Forbush, K.T., Goldberg, D., Hasin, D., Hyman, S.E., Ivanova, M.Y., Lynam, D.R., Markon, K., Miller, J.D., Moffitt, T.E., Morey, L.C., Mullins-Sweatt, S.N., Ormel, J., Patrick, C.J., Regier, D.A., Rescorla, L., Ruggero, C.J., Samuel, D.B., Sellbom, M., Simms, L.J., Skodol, A.E., Slade, T., South, S.C., Tackett, J.L., Waldman, I.D., Waszczuk, M.A., Widiger, T.A., Wright, A.G.C., Zimmerman, M., 2017. The Hierarchical Taxonomy of Psychopathology (HiTOP): A dimensional alternative to traditional nosologies. J. Abnorm. Psychol. 126, 454–477. https://doi.org/10.1037/abn0000258

Lahey, B.B., Applegate, B., Hakes, J.K., Zald, D.H., Hariri, A.R., Rathouz, P.J., 2012. Is there a general factor of prevalent psychopathology during adulthood? J. Abnorm. Psychol. 121, 971–977. https://doi.org/10.1037/a0028355

Lahey, B.B., Krueger, R.F., Rathouz, P.J., Waldman, I.D., Zald, D.H., 2017. A hierarchical causal taxonomy of psychopathology across the life span. Psychol. Bull. 143, 142.

Lahey, B.B., Van Hulle, C.A., Singh, A.L., Waldman, I.D., Rathouz, P.J., 2011. Higher-order genetic and environmental structure of prevalent forms of child and adolescent psychopathology. Arch. Gen. Psychiatry 68, 181–189. https://doi.org/10.1001/archgenpsychiatry.2010.192

Leban, L., 2021. The Effects of Adverse Childhood Experiences and Gender on Developmental Trajectories of Internalizing and Externalizing Outcomes. Crime Delinquency 67, 631–661. https://doi.org/10.1177/0011128721989059

Lebel, C., Beaulieu, C., 2011. Longitudinal Development of Human Brain Wiring Continues from Childhood into Adulthood. J. Neurosci. 31, 10937–10947. https://doi.org/10.1523/JNEUROSCI.5302-10.2011

Lee, P.H., Anttila, V., Won, H., Feng, Y.-C.A., Rosenthal, J., Zhu, Z., Tucker-Drob, E.M., Nivard, M.G., Grotzinger, A.D., Posthuma, D., Wang, M.M.-J., Yu, D., Stahl, E.A., Walters, R.K., Anney, R.J.L., Duncan, L.E., Ge, T., Adolfsson, R., Banaschewski, T., Belangero, S., Cook, E.H., Coppola, G., Derks, E.M., Hoekstra, P.J., Kaprio, J., Keski-Rahkonen, A., Kirov, G., Kranzler, H.R., Luykx, J.J., Rohde, L.A., Zai, C.C., Agerbo, E., Arranz, M.J., Asherson, P., Bækvad-Hansen, M., Baldursson, G., Bellgrove, M., Belliveau, R.A., Buitelaar, J., Burton, C.L., Bybjerg-Grauholm, J., Casas, M., Cerrato, F., Chambert, K., Churchhouse, C., Cormand, B., Crosbie, J., Dalsgaard, S., Demontis, D., Doyle, A.E., Dumont, A., Elia, J., Grove, J., Gudmundsson, O.O., Haavik, J., Hakonarson, H., Hansen, C.S., Hartman, C.A., Hawi, Z., Hervás, A., Hougaard, D.M., Howrigan, D.P., Huang, H., Kuntsi, J., Langley, K.,

Lesch, K.-P., Leung, P.W.L., Loo, S.K., Martin, J., Martin, A.R., McGough, J.J., Medland, S.E., Moran, J.L., Mors, O., Mortensen, P.B., Oades, R.D., Palmer, D.S., Pedersen, C.B., Pedersen, M.G., Peters, T., Poterba, T., Poulsen, J.B., Ramos-Quiroga, J.A., Reif, A., Ribasés, M., Rothenberger, A., Rovira, P., Sánchez-Mora, C., Satterstrom, F.K., Schachar, R., Artigas, M.S., Steinberg, S., Stefansson, H., Turley, P., Walters, G.B., Werge, T., Zayats, T., Arking, D.E., Bettella, F., Buxbaum, J.D., Christensen, J.H., Collins, R.L., Coon, H., De Rubeis, S., Delorme, R., Grice, D.E., Hansen, T.F., Holmans, P.A., Hope, S., Hultman, C.M., Klei, L., Ladd-Acosta, C., Magnusson, P., Nærland, T., Nyegaard, M., Pinto, D., Qvist, P., Rehnström, K., Reichenberg, A., Reichert, J., Roeder, K., Rouleau, G.A., Saemundsen, E., Sanders, S.J., Sandin, S., St Pourcain, B., Stefansson, K., Sutcliffe, J.S., Talkowski, M.E., Weiss, L.A., Willsey, A.J., Agartz, I., Akil, H., Albani, D., Alda, M., Als, T.D., Anjorin, A., Backlund, L., Bass, N., Bauer, M., Baune, B.T., Bellivier, F., Bergen, S.E., Berrettini, W.H., Biernacka, J.M., Blackwood, D.H.R., Bøen, E., Budde, M., Bunney, W., Burmeister, M., Byerley, W., Byrne, E.M., Cichon, S., Clarke, T.-K., Coleman, J.R.I., Craddock, N., Curtis, D., Czerski, P.M., Dale, A.M., Dalkner, N., Dannlowski, U., Degenhardt, F., Di Florio, A., Elvsåshagen, T., Etain, B., Fischer, S.B., Forstner, A.J., Forty, L., Frank, J., Frye, M., Fullerton, J.M., Gade, K., Gaspar, H.A., Gershon, E.S., Gill, M., Goes, F.S., Gordon, S.D., Gordon-Smith, K., Green, M.J., Greenwood, T.A., Grigoroiu-Serbanescu, M., Guzman-Parra, J., Hauser, J., Hautzinger, M., Heilbronner, U., Herms, S., Hoffmann, P., Holland, D., Jamain, S., Jones, I., Jones, L.A., Kandaswamy, R., Kelsoe, J.R., Kennedy, J.L., Joachim, O.K., Kittel-Schneider, S., Kogevinas, M., Koller, A.C., Lavebratt, C., Lewis, C.M., Li, Q.S., Lissowska, J., Loohuis, L.M.O., Lucae, S., Maaser, A., Malt, U.F., Martin, N.G., Martinsson, L., McElroy, S.L., McMahon, F.J., McQuillin, A., Melle, I., Metspalu, A., Millischer, V., Mitchell, P.B., Montgomery, G.W., Morken, G., Morris, D.W., Müller-Myhsok, B., Mullins, N., Myers, R.M., Nievergelt, C.M., Nordentoft, M., Adolfsson, A.N., Nöthen, M.M., Ophoff, R.A., Owen, M.J., Paciga, S.A., Pato, C.N., Pato, M.T., Perlis, R.H., Perry, A., Potash, J.B., Reinbold, C.S., Rietschel, M., Rivera, M., Roberson, M., Schalling, M., Schofield, P.R., Schulze, T.G., Scott, L.J., Serretti, A., Sigurdsson, E., Smeland, O.B., Stordal, E., Streit, F., Strohmaier, J., Thorgeirsson, T.E., Treutlein, J., Turecki, G., Vaaler, A.E., Vieta, E., Vincent, J.B., Wang, Y., Witt, S.H., Zandi, P., Adan, R.A.H., Alfredsson, L., Ando, T., Aschauer, H., Baker, J.H., Bencko, V., Bergen, A.W., Birgegård, A., Perica, V.B., Brandt, H., Burghardt, R., Carlberg, L., Cassina, M., Clementi, M., Courtet, P., Crawford, S., Crow, S., Crowley, J.J., Danner, U.N., Davis, O.S.P., Degortes, D., DeSocio, J.E., Dick, D.M., Dina, C., Docampo, E., Egberts, K., Ehrlich, S., Espeseth, T., Fernández-Aranda, F., Fichter, M.M., Foretova, L., Forzan, M., Gambaro, G., Giegling, I., Gonidakis, F., Gorwood, P., Mayora, M.G., Guo, Y., Halmi, K.A., Hatzikotoulas, K., Hebebrand, J., Helder, S.G., Herpertz-Dahlmann, B., Herzog, W., Hinney, A., Imgart, H., Jiménez-Murcia, S., Johnson, C., Jordan, J., Julià, A., Kaminská, D., Karhunen, L., Karwautz, A., Kas, M.J.H., Kaye, W.H., Kennedy, M.A., Kim, Y.-R., Klareskog, L., Klump, K.L., Knudsen, G.P.S., Landén, M., Le Hellard, S., Levitan, R.D., Li, D., Lichtenstein, P., Maj, M., Marsal, S., McDevitt, S., Mitchell, J., Monteleone, P.,

Monteleone, A.M., Munn-Chernoff, M.A., Nacmias, B., Navratilova, M., O'Toole, J.K., Padyukov, L., Pantel, J., Papezova, H., Rabionet, R., Raevuori, A., Ramoz, N., Reichborn-Kjennerud, T., Ricca, V., Roberts, M., Rujescu, D., Rybakowski, F., Scherag, A., Schmidt, U., Seitz, J., Slachtova, L., Slof-Op't Landt, M.C.T., Slopien, A., Sorbi, S., Southam, L., Strober, M., Tortorella, A., Tozzi, F., Treasure, J., Tziouvas, K., van Elburg, A.A., Wade, T.D., Wagner, G., Walton, E., Watson, H.J., Wichmann, H.-E., Woodside, D.B., Zeggini, E., Zerwas, S., Zipfel, S., Adams, M.J., Andlauer, T.F.M., Berger, K., Binder, E.B., Boomsma, D.I., Castelao, E., Colodro-Conde, L., Direk, N., Docherty, A.R., Domenici, E., Domschke, K., Dunn, E.C., Foo, J.C., de. Geus, E.J.C., Grabe, H.J., Hamilton, S.P., Horn, C., Hottenga, J.-J., Howard, D., Ising, M., Kloiber, S., Levinson, D.F., Lewis, G., Magnusson, P.K.E., Mbarek, H., Middeldorp, C.M., Mostafavi, S., Nyholt, D.R., Penninx, B.WJH., Peterson, R.E., Pistis, G., Porteous, D.J., Preisig, M., Quiroz, J.A., Schaefer, C., Schulte, E.C., Shi, J., Smith, D.J., Thomson, P.A., Tiemeier, H., Uher, R., van der Auwera, S., Weissman, M.M., Alexander, M., Begemann, M., Bramon, E., Buccola, N.G., Cairns, M.J., Campion, D., Carr, V.J., Cloninger, C.R., Cohen, D., Collier, D.A., Corvin, A., DeLisi, L.E., Donohoe, G., Dudbridge, F., Duan, J., Freedman, R., Gejman, P.V., Golimbet, V., Godard, S., Ehrenreich, H., Hartmann, A.M., Henskens, F.A., Ikeda, M., Iwata, N., Jablensky, A.V., Joa, I., Jönsson, E.G., Kelly, B.J., Knight, J., Konte, B., Laurent-Levinson, C., Lee, J., Lencz, T., Lerer, B., Loughland, C.M., Malhotra, A.K., Mallet, J., McDonald, C., Mitjans, M., Mowry, B.J., Murphy, K.C., Murray, R.M., O'Neill, F.A., Oh, S.-Y., Palotie, A., Pantelis, C., Pulver, A.E., Petryshen, T.L., Quested, D.J., Riley, B., Sanders, A.R., Schall, U., Schwab, S.G., Scott, R.J., Sham, P.C., Silverman, J.M., Sim, K., Steixner, A.A., Tooney, P.A., van Os, J., Vawter, M.P., Walsh, D., Weiser, M., Wildenauer, D.B., Williams, N.M., Wormley, B.K., Zhang, F., Androutsos, C., Arnold, P.D., Barr, C.L., Barta, C., Bey, K., Bienvenu, O.J., Black, D.W., Brown, L.W., Budman, C., Cath, D., Cheon, K.-A., Ciullo, V., Coffey, B.J., Cusi, D., Davis, L.K., Denys, D., Depienne, C., Dietrich, A., Eapen, V., Falkai, P., Fernandez, T.V., Garcia-Delgar, B., Geller, D.A., Gilbert, D.L., Grados, M.A., Greenberg, E., Grünblatt, E., Hagstrøm, J., Hanna, G.L., Hartmann, A., Hedderly, T., Heiman, G.A., Heyman, I., Hong, H.J., Huang, A., Huyser, C., Ibanez-Gomez, L., Khramtsova, E.A., Kim, Y.K., Kim, Y.-S., King, R.A., Koh, Y.-J., Konstantinidis, A., Kook, S., Kuperman, S., Leventhal, B.L., Lochner, C., Ludolph, A.G., Madruga-Garrido, M., Malaty, I., Maras, A., McCracken, J.T., Meijer, I.A., Mir, P., Morer, A., Müller-Vahl, K.R., Münchau, A., Murphy, T.L., Naarden, A., Nagy, P., Nestadt, G., Nestadt, P.S., Nicolini, H., Nurmi, E.L., Okun, M.S., Paschou, P., Piras, Fabrizio, Piras, Federica, Pittenger, C., Plessen, K.J., Richter, M.A., Rizzo, R., Robertson, M., Roessner, V., Ruhrmann, S., Samuels, J.F., Sandor, P., Schlögelhofer, M., Shin, E.-Y., Singer, H., Song, D.-H., Song, J., Spalletta, G., Stein, D.J., Stewart, S.E., Storch, E.A., Stranger, B., Stuhrmann, M., Tarnok, Z., Tischfield, J.A., Tübing, J., Visscher, F., Vulink, N., Wagner, M., Walitza, S., Wanderer, S., Woods, M., Worbe, Y., Zai, G., Zinner, S.H., Sullivan, P.F., Franke, B., Daly, M.J., Bulik, C.M., Lewis, C.M., McIntosh, A.M., O'Donovan, M.C., Zheutlin, A., Andreassen, O.A., Børglum, A.D., Breen, G., Edenberg, H.J., Fanous, A.H., Faraone,

S.V., Gelernter, J., Mathews, C.A., Mattheisen, M., Mitchell, K.S., Neale, M.C., Nurnberger, J.I., Ripke, S., Santangelo, S.L., Scharf, J.M., Stein, M.B., Thornton, L.M., Walters, J.T.R., Wray, N.R., Geschwind, D.H., Neale, B.M., Kendler, K.S., Smoller, J.W., 2019. Genomic Relationships, Novel Loci, and Pleiotropic Mechanisms across Eight Psychiatric Disorders. Cell 179, 1469-1482.e11. https://doi.org/10.1016/j.cell.2019.11.020

Lundström, S., Chang, Z., Råstam, M., Gillberg, C., Larsson, H., Anckarsäter, H., Lichtenstein, P., 2012. Autism Spectrum Disorders and Autisticlike Traits: Similar Etiology in the Extreme End and the Normal Variation. Arch. Gen. Psychiatry 69, 46–52. https://doi.org/10.1001/archgenpsychiatry.2011.144

Lynch, S.J., Sunderland, M., Newton, N.C., Chapman, C., 2021. A systematic review of transdiagnostic risk and protective factors for general and specific psychopathology in young people. Clin. Psychol. Rev. 87, 102036. https://doi.org/10.1016/j.cpr.2021.102036

Margulies, D.S., Ghosh, S.S., Goulas, A., Falkiewicz, M., Huntenburg, J.M., Langs, G., Bezgin, G., Eickhoff, S.B., Castellanos, F.X., Petrides, M., Jefferies, E., Smallwood, J., 2016. Situating the default-mode network along a principal gradient of macroscale cortical organization. Proc. Natl. Acad. Sci. 113, 12574–12579. https://doi.org/10.1073/pnas.1608282113

McIntosh, A.R., Lobaugh, N.J., 2004. Partial least squares analysis of neuroimaging data: applications and advances. NeuroImage 23 Suppl 1, S250-263. https://doi.org/10.1016/j.neuroimage.2004.07.020

McIntosh, A.R., Mišić, B., 2013. Multivariate statistical analyses for neuroimaging data. Annu. Rev. Psychol. 64, 499–525. https://doi.org/10.1146/annurev-psych-113011-143804

Mesulam, M.M., 1998. From sensation to cognition. Brain 121, 1013–1052. https://doi.org/10.1093/brain/121.6.1013

Michelini, G., Barch, D.M., Tian, Y., Watson, D., Klein, D.N., Kotov, R., 2019. Delineating and validating higher-order dimensions of psychopathology in the Adolescent Brain Cognitive Development (ABCD) study. Transl. Psychiatry 9, 1–15. https://doi.org/10.1038/s41398-019-0593-4

Michelini, G., Cheung, C.H.M., Kitsune, V., Brandeis, D., Banaschewski, T., McLoughlin, G., Asherson, P., Rijsdijk, F., Kuntsi, J., 2021. The Etiological Structure of Cognitive-Neurophysiological Impairments in ADHD in Adolescence and Young Adulthood. J. Atten. Disord. 25, 91–104. https://doi.org/10.1177/1087054718771191

Miller, K.L., Alfaro-Almagro, F., Bangerter, N.K., Thomas, D.L., Yacoub, E., Xu, J., Bartsch, A.J., Jbabdi, S., Sotiropoulos, S.N., Andersson, J.L.R., Griffanti, L., Douaud,

G., Okell, T.W., Weale, P., Dragonu, I., Garratt, S., Hudson, S., Collins, R., Jenkinson, M., Matthews, P.M., Smith, S.M., 2016. Multimodal population brain imaging in the UK Biobank prospective epidemiological study. Nat. Neurosci. 19, 1523–1536. https://doi.org/10.1038/nn.4393

Mills, K.L., Siegmund, K.D., Tamnes, C.K., Ferschmann, L., Wierenga, L.M., Bos, M.G.N., Luna, B., Li, C., Herting, M.M., 2021. Inter-individual variability in structural brain development from late childhood to young adulthood. NeuroImage 118450. https://doi.org/10.1016/j.neuroimage.2021.118450

Modabbernia, A., Michelini, G., Reichenberg, A., Kotov, R., Barch, D., Frangou, S., 2022. Neural Signatures of Data-Driven Psychopathology Dimensions at the Transition to Adolescence. Eur. Psychiatry 1–27. https://doi.org/10.1192/j.eurpsy.2021.2262

Opel, N., Goltermann, J., Hermesdorf, M., Berger, K., Baune, B.T., Dannlowski, U., 2020. Cross-Disorder Analysis of Brain Structural Abnormalities in Six Major Psychiatric Disorders: A Secondary Analysis of Mega- and Meta-analytical Findings From the ENIGMA Consortium. Biol. Psychiatry, New Mechanisms of Psychosis: Clinical Implications 88, 678–686. https://doi.org/10.1016/j.biopsych.2020.04.027

Paquola, C., Seidlitz, J., Benkarim, O., Royer, J., Klimes, P., Bethlehem, R.A.I., Larivière, S., Wael, R.V. de, Rodríguez-Cruces, R., Hall, J.A., Frauscher, B., Smallwood, J., Bernhardt, B.C., 2020. A multi-scale cortical wiring space links cellular architecture and functional dynamics in the human brain. PLOS Biol. 18, e3000979. https://doi.org/10.1371/journal.pbio.3000979

Paquola, C., Wael, R.V.D., Wagstyl, K., Bethlehem, R.A.I., Hong, S.-J., Seidlitz, J., Bullmore, E.T., Evans, A.C., Misic, B., Margulies, D.S., Smallwood, J., Bernhardt, B.C., 2019. Microstructural and functional gradients are increasingly dissociated in transmodal cortices. PLOS Biol. 17, e3000284. https://doi.org/10.1371/journal.pbio.3000284

Park, B., Kebets, V., Larivière, S., Hettwer, M.D., Paquola, C., van Rooij, D., Buitelaar, J., Franke, B., Hoogman, M., Schmaal, L., Veltman, D.J., van den Heuvel, O.A., Stein, D.J., Andreassen, O.A., Ching, C.R.K., Turner, J.A., van Erp, T.G.M., Evans, A.C., Dagher, A., Thomopoulos, S.I., Thompson, P.M., Valk, S.L., Kirschner, M., Bernhardt, B.C., 2022a. Multiscale neural gradients reflect transdiagnostic effects of major psychiatric conditions on cortical morphology. Commun. Biol. 5, 1–14. https://doi.org/10.1038/s42003-022-03963-z

Park, B., Paquola, C., Bethlehem, R.A., Benkarim, O., Consortium, N. in P.N. (NSPN), Mišić, B., Smallwood, J., Bullmore, E.T., Bernhardt, B.C., 2022b. Adolescent development of multiscale structural wiring and functional interactions in the human connectome. Proc. Natl. Acad. Sci. 119, e2116673119.

Parkes, L., Moore, T.M., Calkins, M.E., Cook, P.A., Cieslak, M., Roalf, D.R., Wolf, D.H., Gur, R.C., Gur, R.E., Satterthwaite, T.D., Bassett, D.S., 2021. Transdiagnostic dimensions of psychopathology explain individuals' unique deviations from normative neurodevelopment in brain structure. Transl. Psychiatry 11, 1–13. https://doi.org/10.1038/s41398-021-01342-6

Parkes, L., Satterthwaite, T.D., Bassett, D.S., 2020. Towards precise resting-state fMRI biomarkers in psychiatry: synthesizing developments in transdiagnostic research, dimensional models of psychopathology, and normative neurodevelopment. Curr. Opin. Neurobiol., Whole-brain interactions between neural circuits 65, 120–128. https://doi.org/10.1016/j.conb.2020.10.016

Paus, T., Keshavan, M., Giedd, J.N., 2008. Why do many psychiatric disorders emerge during adolescence? Nat. Rev. Neurosci. 9, 947–957. https://doi.org/10.1038/nrn2513

Pettersson, E., Anckarsäter, H., Gillberg, C., Lichtenstein, P., 2013. Different neurodevelopmental symptoms have a common genetic etiology. J. Child Psychol. Psychiatry 54, 1356–1365. https://doi.org/10.1111/jcpp.12113

Pettersson, E., Larsson, H., Lichtenstein, P., 2016. Common psychiatric disorders share the same genetic origin: a multivariate sibling study of the Swedish population. Mol. Psychiatry 21, 717–721. https://doi.org/10.1038/mp.2015.116

Plomin, R., Haworth, C.M.A., Davis, O.S.P., 2009. Common disorders are quantitative traits. Nat. Rev. Genet. 10, 872–878. https://doi.org/10.1038/nrg2670

Raznahan, A., Shaw, P., Lalonde, F., Stockman, M., Wallace, G.L., Greenstein, D., Clasen, L., Gogtay, N., Giedd, J.N., 2011. How Does Your Cortex Grow? J. Neurosci. 31, 7174–7177. https://doi.org/10.1523/JNEUROSCI.0054-11.2011

Robinson, E.B., Koenen, K.C., McCormick, M.C., Munir, K., Hallett, V., Happé, F., Plomin, R., Ronald, A., 2011. Evidence That Autistic Traits Show the Same Etiology in the General Population and at the Quantitative Extremes (5%, 2.5%, and 1%). Arch. Gen. Psychiatry 68, 1113–1121. https://doi.org/10.1001/archgenpsychiatry.2011.119

Robinson, E.B., Pourcain, B.S., Anttila, V., Kosmicki, J.A., Bulik-Sullivan, B., Grove, J., Maller, J., Samocha, K.E., Sanders, S.J., Ripke, S., Martin, J., Hollegaard, M.V., Werge, T., Hougaard, D.M., Neale, B.M., Evans, D.M., Skuse, D., Mortensen, P.B., Børglum, A.D., Ronald, A., Smith, G.D., Daly, M.J., 2016. Genetic risk for autism spectrum disorders and neuropsychiatric variation in the general population. Nat. Genet. 48, 552–555. https://doi.org/10.1038/ng.3529

Romer, A.L., Elliott, M.L., Knodt, A.R., Sison, M.L., Ireland, D., Houts, R., Ramrakha, S., Poulton, R., Keenan, R., Melzer, T.R., Moffitt, T.E., Caspi, A., Hariri, A.R., 2020. Pervasively Thinner Neocortex as a Transdiagnostic Feature of General

Psychopathology. Am. J. Psychiatry appi.ajp.2020.19090934. https://doi.org/10.1176/appi.ajp.2020.19090934

Romer, A.L., Knodt, A.R., Houts, R., Brigidi, B.D., Moffitt, T.E., Caspi, A., Hariri, A.R., 2018. Structural alterations within cerebellar circuitry are associated with general liability for common mental disorders. Mol. Psychiatry 23, 1084–1090. https://doi.org/10.1038/mp.2017.57

Romer, A.L., Pizzagalli, D.A., 2021. Associations between Brain Structural Alterations, Executive Dysfunction, and General Psychopathology in a Healthy and Cross-Diagnostic Adult Patient Sample. Biol. Psychiatry Glob. Open Sci. https://doi.org/10.1016/j.bpsgos.2021.06.002

Ronald, A., Simonoff, E., Kuntsi, J., Asherson, P., Plomin, R., 2008. Evidence for overlapping genetic influences on autistic and ADHD behaviours in a community twin sample. J. Child Psychol. Psychiatry 49, 535–542. https://doi.org/10.1111/j.1469-7610.2007.01857.x

Royer, J., Rodríguez-Cruces, R., Tavakol, S., Larivière, S., Herholz, P., Li, Q., Vos de Wael, R., Paquola, C., Benkarim, O., Park, B., Lowe, A.J., Margulies, D., Smallwood, J., Bernasconi, A., Bernasconi, N., Frauscher, B., Bernhardt, B.C., 2022. An Open MRI Dataset For Multiscale Neuroscience. Sci. Data 9, 569. https://doi.org/10.1038/s41597-022-01682-y

Satterthwaite, T.D., Connolly, J.J., Ruparel, K., Calkins, M.E., Jackson, C., Elliott, M.A., Roalf, D.R., Hopson, R., Prabhakaran, K., Behr, M., Qiu, H., Mentch, F.D., Chiavacci, R., Sleiman, P.M.A., Gur, R.C., Hakonarson, H., Gur, R.E., 2016. The Philadelphia Neurodevelopmental Cohort: A publicly available resource for the study of normal and abnormal brain development in youth. NeuroImage, Sharing the wealth: Brain Imaging Repositories in 2015 124, 1115–1119. https://doi.org/10.1016/j.neuroimage.2015.03.056

Schaefer, A., Kong, R., Gordon, E.M., Laumann, T.O., Zuo, X.-N., Holmes, A.J., Eickhoff, S.B., Yeo, B.T.T., 2018. Local-Global Parcellation of the Human Cerebral Cortex from Intrinsic Functional Connectivity MRI. Cereb. Cortex 28, 3095–3114. https://doi.org/10.1093/cercor/bhx179

Ségonne, F., Dale, A.M., Busa, E., Glessner, M., Salat, D., Hahn, H.K., Fischl, B., 2004. A hybrid approach to the skull stripping problem in MRI. NeuroImage 22, 1060–1075. https://doi.org/10.1016/j.neuroimage.2004.03.032

Ségonne, F., Pacheco, J., Fischl, B., 2007. Geometrically accurate topology-correction of cortical surfaces using nonseparating loops. IEEE Trans. Med. Imaging 26, 518–529. https://doi.org/10.1109/TMI.2006.887364

Sha, Z., Xia, M., Lin, Q., Cao, M., Tang, Y., Xu, K., Song, H., Wang, Z., Wang, F., Fox, P.T., Evans, A.C., He, Y., 2018. Meta-Connectomic Analysis Reveals Commonly Disrupted Functional Architectures in Network Modules and Connectors across Brain Disorders. Cereb. Cortex 28, 4179–4194. https://doi.org/10.1093/cercor/bhx273

Shanmugan, S., Wolf, D.H., Calkins, M.E., Moore, T.M., Ruparel, K., Hopson, R.D., Vandekar, S.N., Roalf, D.R., Elliott, M.A., Jackson, C., Gennatas, E.D., Leibenluft, E., Pine, D.S., Shinohara, R.T., Hakonarson, H., Gur, R.C., Gur, R.E., Satterthwaite, T.D., 2016. Common and Dissociable Mechanisms of Executive System Dysfunction Across Psychiatric Disorders in Youth. Am. J. Psychiatry 173, 517–526. https://doi.org/10.1176/appi.ajp.2015.15060725

Shen, X., MacSweeney, N., Chan, S.W.Y., Barbu, M.C., Adams, M.J., Lawrie, S.M., Romaniuk, L., McIntosh, A.M., Whalley, H.C., 2021. Brain structural associations with depression in a large early adolescent sample (the ABCD study®). EClinicalMedicine 42, 101204. https://doi.org/10.1016/j.eclinm.2021.101204

Siugzdaite, R., Bathelt, J., Holmes, J., Astle, D.E., 2020. Transdiagnostic Brain Mapping in Developmental Disorders. Curr. Biol. 30, 1245-1257.e4. https://doi.org/10.1016/j.cub.2020.01.078

Solmi, M., Radua, J., Olivola, M., Croce, E., Soardo, L., Salazar de Pablo, G., Il Shin, J., Kirkbride, J.B., Jones, P., Kim, J.H., Kim, J.Y., Carvalho, A.F., Seeman, M.V., Correll, C.U., Fusar-Poli, P., 2022. Age at onset of mental disorders worldwide: large-scale meta-analysis of 192 epidemiological studies. Mol. Psychiatry 27, 281–295. https://doi.org/10.1038/s41380-021-01161-7

Sprooten, E., Franke, B., Greven, C.U., 2021. The P-factor and its genomic and neural equivalents: an integrated perspective. Mol. Psychiatry 1–11. https://doi.org/10.1038/s41380-021-01031-2

Sydnor, V.J., Larsen, B., Bassett, D.S., Alexander-Bloch, A., Fair, D.A., Liston, C., Mackey, A.P., Milham, M.P., Pines, A., Roalf, D.R., Seidlitz, J., Xu, T., Raznahan, A., Satterthwaite, T.D., 2021. Neurodevelopment of the association cortices: Patterns, mechanisms, and implications for psychopathology. Neuron 109, 2820–2846. https://doi.org/10.1016/j.neuron.2021.06.016

Thompson, P.M., Stein, J.L., Medland, S.E., Hibar, D.P., Vasquez, A.A., Renteria, M.E., Toro, R., Jahanshad, N., Schumann, G., Franke, B., Wright, M.J., Martin, N.G., Agartz, I., Alda, M., Alhusaini, S., Almasy, L., Almeida, J., Alpert, K., Andreasen, N.C., Andreassen, O.A., Apostolova, L.G., Appel, K., Armstrong, N.J., Aribisala, B., Bastin, M.E., Bauer, M., Bearden, C.E., Bergmann, Ø., Binder, E.B., Blangero, J., Bockholt, H.J., Bøen, E., Bois, C., Boomsma, D.I., Booth, T., Bowman, I.J., Bralten, J., Brouwer, R.M., Brunner, H.G., Brohawn, D.G., Buckner, R.L., Buitelaar, J., Bulayeva, K., Bustillo, J.R., Calhoun, V.D., Cannon, D.M., Cantor, R.M., Carless,

M.A., Caseras, X., Cavalleri, G.L., Chakravarty, M.M., Chang, K.D., Ching, C.R.K., Christoforou, A., Cichon, S., Clark, V.P., Conrod, P., Coppola, G., Crespo-Facorro, B., Curran, J.E., Czisch, M., Deary, I.J., de Geus, E.J.C., den Braber, A., Delvecchio, G., Depondt, C., de Haan, L., de Zubicaray, G.I., Dima, D., Dimitrova, R., Djurovic, S., Dong, H., Donohoe, G., Duggirala, R., Dyer, T.D., Ehrlich, S., Ekman, C.J., Elvsåshagen, T., Emsell, L., Erk, S., Espeseth, T., Fagerness, J., Fears, S., Fedko, I., Fernández, G., Fisher, S.E., Foroud, T., Fox, P.T., Francks, C., Frangou, S., Frey, E.M., Frodl, T., Frouin, V., Garavan, H., Giddaluru, S., Glahn, D.C., Godlewska, B., Goldstein, R.Z., Gollub, R.L., Grabe, H.J., Grimm, O., Gruber, O., Guadalupe, T., Gur, R.E., Gur, R.C., Göring, H.H.H., Hagenaars, S., Hajek, T., Hall, G.B., Hall, J., Hardy, J., Hartman, C.A., Hass, J., Hatton, S.N., Haukvik, U.K., Hegenscheid, K., Heinz, A., Hickie, I.B., Ho, B.-C., Hoehn, D., Hoekstra, P.J., Hollinshead, M., Holmes, A.J., Homuth, G., Hoogman, M., Hong, L.E., Hosten, N., Hottenga, J.-J., Hulshoff Pol, H.E., Hwang, K.S., Jack, C.R., Jenkinson, M., Johnston, C., Jönsson, E.G., Kahn, R.S., Kasperaviciute, D., Kelly, S., Kim, S., Kochunov, P., Koenders, L., Krämer, B., Kwok, J.B.J., Lagopoulos, J., Laje, G., Landen, M., Landman, B.A., Lauriello, J., Lawrie, S.M., Lee, P.H., Le Hellard, S., Lemaître, H., Leonardo, C.D., Li, C., Liberg, B., Liewald, D.C., Liu, X., Lopez, L.M., Loth, E., Lourdusamy, A., Luciano, M., Macciardi, F., Machielsen, M.W.J., MacQueen, G.M., Malt, U.F., Mandl, R., Manoach, D.S., Martinot, J.-L., Matarin, M., Mather, K.A., Mattheisen, M., Mattingsdal, M., Meyer-Lindenberg, A., McDonald, C., McIntosh, A.M., McMahon, F.J., McMahon, K.L., Meisenzahl, E., Melle, I., Milaneschi, Y., Mohnke, S., Montgomery, G.W., Morris, D.W., Moses, E.K., Mueller, B.A., Muñoz Maniega, S., Mühleisen, T.W., Müller-Myhsok, B., Mwangi, B., Nauck, M., Nho, K., Nichols, T.E., Nilsson, L.-G., Nugent, A.C., Nyberg, L., Olvera, R.L., Oosterlaan, J., Ophoff, R.A., Pandolfo, M., Papalampropoulou-Tsiridou, M., Papmeyer, M., Paus, T., Pausova, Z., Pearlson, G.D., Penninx, B.W., Peterson, C.P., Pfennig, A., Phillips, M., Pike, G.B., Poline, J.-B., Potkin, S.G., Pütz, B., Ramasamy, A., Rasmussen, J., Rietschel, M., Rijpkema, M., Risacher, S.L., Roffman, J.L., Roiz-Santiañez, R., Romanczuk-Seiferth, N., Rose, E.J., Royle, N.A., Rujescu, D., Ryten, M., Sachdev, P.S., Salami, A., Satterthwaite, T.D., Savitz, J., Saykin, A.J., Scanlon, C., Schmaal, L., Schnack, H.G., Schork, A.J., Schulz, S.C., Schür, R., Seidman, L., Shen, L., Shoemaker, J.M., Simmons, A., Sisodiya, S.M., Smith, C., Smoller, J.W., Soares, J.C., Sponheim, S.R., Sprooten, E., Starr, J.M., Steen, V.M., Strakowski, S., Strike, L., Sussmann, J., Sämann, P.G., Teumer, A., Toga, A.W., Tordesillas-Gutierrez, D., Trabzuni, D., Trost, S., Turner, J., Van den Heuvel, M., van der Wee, N.J., van Eijk, K., van Erp, T.G.M., van Haren, N.E.M., van ‘t Ent, D., van Tol, M.-J., Valdés Hernández, M.C., Veltman, D.J., Versace, A., Völzke, H., Walker, R., Walter, H., Wang, L., Wardlaw, J.M., Weale, M.E., Weiner, M.W., Wen, W., Westlye, L.T., Whalley, H.C., Whelan, C.D., White, T., Winkler, A.M., Wittfeld, K., Woldehawariat, G., Wolf, C., Zilles, D., Zwiers, M.P., Thalamuthu, A., Schofield, P.R., Freimer, N.B., Lawrence, N.S., Drevets, W., the Alzheimer’s Disease Neuroimaging Initiative, E.C., IMAGEN Consortium, Saguenay Youth Study (SYS) Group, 2014. The ENIGMA Consortium: large-scale collaborative analyses of

neuroimaging and genetic data. Brain Imaging Behav. 8, 153–182. https://doi.org/10.1007/s11682-013-9269-5

Van Dam, N.T., O'Connor, D., Marcelle, E.T., Ho, E.J., Cameron Craddock, R., Tobe, R.H., Gabbay, V., Hudziak, J.J., Xavier Castellanos, F., Leventhal, B.L., Milham, M.P., 2017. Data-Driven Phenotypic Categorization for Neurobiological Analyses: Beyond DSM-5 Labels. Biol. Psychiatry 81, 484–494. https://doi.org/10.1016/j.biopsych.2016.06.027

Van Essen, D.C., Smith, S.M., Barch, D.M., Behrens, T.E.J., Yacoub, E., Ugurbil, K., 2013. The WU-Minn Human Connectome Project: An overview. NeuroImage, Mapping the Connectome 80, 62–79. https://doi.org/10.1016/j.neuroimage.2013.05.041

Vos de Wael, R., Benkarim, O., Paquola, C., Lariviere, S., Royer, J., Tavakol, S., Xu, T., Hong, S.-J., Valk, S.L., Misic, B., Milham, M.P., Margulies, D.S., Smallwood, J., Bernhardt, B.C., 2020. BrainSpace: a toolbox for the analysis of macroscale gradients in neuroimaging and connectomics datasets. Commun. Biol. 3, 1. https://doi.org/10.1101/761460

Waszczuk, M.A., Miao, J., Docherty, A.R., Shabalin, A.A., Jonas, K.G., Michelini, G., Kotov, R., 2021. General v. specific vulnerabilities: polygenic risk scores and higher-order psychopathology dimensions in the Adolescent Brain Cognitive Development (ABCD) Study. Psychol. Med. 1–10. https://doi.org/10.1017/S0033291721003639

Xia, C.H., Ma, Z., Ciric, R., Gu, S., Betzel, R.F., Kaczkurkin, A.N., Calkins, M.E., Cook, P.A., García de la Garza, A., Vandekar, S.N., Cui, Z., Moore, T.M., Roalf, D.R., Ruparel, K., Wolf, D.H., Davatzikos, C., Gur, R.C., Gur, R.E., Shinohara, R.T., Bassett, D.S., Satterthwaite, T.D., 2018. Linked dimensions of psychopathology and connectivity in functional brain networks. Nat. Commun. 9, 3003. https://doi.org/10.1038/s41467-018-05317-y

Yeo, B.T.T., Krienen, F.M., Sepulcre, J., Sabuncu, M.R., Lashkari, D., Hollinshead, M., Roffman, J.L., Smoller, J.W., Zöllei, L., Polimeni, J.R., Fischl, B., Liu, H., Buckner, R.L., 2011. The organization of the human cerebral cortex estimated by intrinsic functional connectivity. J. Neurophysiol. 106, 1125–1165. https://doi.org/10.1152/jn.00338.2011